

Differential Gene Expression in *Arabidopsis thaliana* in Response to
Methyljasmonate and 12-Hydroxyjasmonate Treatments

Irina Gaber

A Thesis In
The Department Of Biology

Presented in Partial Fulfillment of the Requirementf for the
Degree of Masters of Science (Biology) at

Concordia University
Montreal, Quebec, Canada

July 2008

© Irina Gaber, 2008



Library and
Archives Canada

Published Heritage
Branch

395 Wellington Street
Ottawa ON K1A 0N4
Canada

Bibliothèque et
Archives Canada

Direction du
Patrimoine de l'édition

395, rue Wellington
Ottawa ON K1A 0N4
Canada

Your file Votre référence
ISBN: 978-0-494-45463-3
Our file Notre référence
ISBN: 978-0-494-45463-3

NOTICE:

The author has granted a non-exclusive license allowing Library and Archives Canada to reproduce, publish, archive, preserve, conserve, communicate to the public by telecommunication or on the Internet, loan, distribute and sell theses worldwide, for commercial or non-commercial purposes, in microform, paper, electronic and/or any other formats.

The author retains copyright ownership and moral rights in this thesis. Neither the thesis nor substantial extracts from it may be printed or otherwise reproduced without the author's permission.

AVIS:

L'auteur a accordé une licence non exclusive permettant à la Bibliothèque et Archives Canada de reproduire, publier, archiver, sauvegarder, conserver, transmettre au public par télécommunication ou par l'Internet, prêter, distribuer et vendre des thèses partout dans le monde, à des fins commerciales ou autres, sur support microforme, papier, électronique et/ou autres formats.

L'auteur conserve la propriété du droit d'auteur et des droits moraux qui protègent cette thèse. Ni la thèse ni des extraits substantiels de celle-ci ne doivent être imprimés ou autrement reproduits sans son autorisation.

In compliance with the Canadian Privacy Act some supporting forms may have been removed from this thesis.

Conformément à la loi canadienne sur la protection de la vie privée, quelques formulaires secondaires ont été enlevés de cette thèse.

While these forms may be included in the document page count, their removal does not represent any loss of content from the thesis.

Bien que ces formulaires aient inclus dans la pagination, il n'y aura aucun contenu manquant.


Canada

ABSTRACT

Differential Gene Expression in *Arabidopsis thaliana* in Response to Methyljasmonate and 12-Hydroxyjasmonate Treatments

Irina Gaber

Jasmonic acid (JA) and its derivatives occur naturally in *Arabidopsis thaliana* (*A. thaliana*), and regulate the expression of a number of genes such as the ones involved in flowering, defence response and senescence. Additionally, precursors and downstream components of the JA pathway have been shown to elicit some of the responses previously attributed to JA. Of interest to our lab was to investigate the effect of a compound downstream of JA, 12-hydroxyjasmonate (12-OHJA), on gene expression as well as the phenotypic effect of accumulating higher internal levels of the compound. This was based on previous data showing that, while most genes are co-regulated by JA and 12-OHJA, *Thi2.1*, one of the marker genes of JA induction, is not upregulated upon 12-OHJA treatment. Furthermore, exogenous application of this compound shares only some of the phenotypes of JA. In order to gain further insight into the molecular function of the two compounds, we investigated the effects of 4h treatments with each compound on gene expression using the Affymetrix® *A. thaliana* full genome array. The data demonstrates that there are subsets of genes that are specifically induced or repressed by each of the two compounds, pointing to the possibility of two differentially regulated pathways.

12-OHJA was recently shown to be sulfonated in vitro by one of the eighteen *A. thaliana* sulfotransferases, *AtST2a* (Gidda *et al*, 2003). To gain further insight of the function of *AtST2a* and its homologous gene *AtST2b* (whose substrate is yet to be identified), knockout plants in each of the genes were

isolated and subjected to phenotypic analyses. The results demonstrate that the *AtST2b*-KO mutant flowers earlier and has more leaves than wildtype or *AtST2a*-KO under short days. Combined with metabolite analysis of mutants, the data suggests that another compound, maybe an isomer of 12-OHJA, is responsible for the control of flowering time in short days.

Dragă Ducu,

*Te port cu mine in fiecare gest, in fiecare zii.
Te iubesc, frațioare!*

Table of Contents

List of Figures	x
List of tables	xiii
List of Abbreviations	xv
1.0 Introduction	1
1.1 Plant life and Flowering: An Introduction	3
1.2 The Switch to Flowering	4
1.3 Early and late flowering mutants and gene identification	5
1.4 Flowering Time Genes	6
1.4.1 The photoperiod pathway	6
1.4.1.1 Long day path.....	8
1.4.1.2 Short day path (Gibberellin pathway)	11
1.4.2 Autonomous pathway	11
1.5 Leaf to Shoot: the 'Florigen' story	12
1.6 Jasmonic Acid and its Known Roles.....	17
1.6.1 Introduction	17
1.6.1.1 Seed Germination and Growth.....	18
1.6.1.2 Vegetative Storage Proteins and Sinks	18
1.6.1.3 Photosynthesis and Senescence	19
1.6.1.4 Insect and Disease Resistance	19
1.6.1.5 JA in flowering	20
1.7 JA Biosynthesis	21
1.7.1 The Jasmonate Pathway	21

1.7.2 JA metabolites	24
1.8 Sulfotransferases and the Sulfonation Reaction	28
1.8.1 Roles of Sulfonation	28
1.8.2 A. thaliana Sulfotransferases	28
1.8.3 The A. thaliana AtST2 Subgroup and its Regulation	29
1.8.4 12-hydroxyjasmonate as a Signalling Molecule	29
1.9 Purpose of Current Work	30
2.0 Materials and Methods	31
2.1 Materials	31
2.2 Methods.....	32
2.2.1 Microarray experiment.....	32
2.2.1.1 Seed sterilization and plant growth	32
2.2.1.2 RNA extraction	32
2.2.1.3 Microarray analysis using the A. thaliana ATH1 Genome Array ...	34
2.2.1.4 Data analysis	34
2.2.2 Reverse-Transcription PCR	37
2.2.3 Phenotype analysis	38
2.2.3.1 Plant growth conditions	38
2.2.3.2 Genomic DNA extraction	38
2.2.3.3 Confirmation of homozygous mutants	39
2.2.3.4 Methyljasmonate and 12-Hydroxyjasmonate Treatments	40
2.2.4 Gene expression analysis of AtST2a and AtST2b KOs	40
2.2.5 Mass spectrometry	41

2.2.5.1 HPLC fractionation of wildtype, AtST2a and AtST2b extracts	41
2.2.5.2 Neutral loss mass spectrometry of purified metabolites from wildtype, AtST2a and AtST2b extracts	42
3.0 Results	44
3.1 Effect of MeJA and 12-OHJA on gene expression.....	44
3.1.1 Introduction	44
3.1.2 Microarray analysis	45
3.1.3 RT-PCR validation of microarray data	56
3.1.4 Biological functions of various clusters	58
3.2 Positioning of the AtST2a and AtST2b genes in the floral pathway	62
3.3 Molecular and phenotypic characterization of AtST2a and AtST2b knockout lines	64
3.3.1 Introduction	64
3.3.2 Molecular characterization of AtSt2a and AtSt2b KO lines	65
3.3.3 Genetic analysis of AtST2a-KO and AtST2b-KO	66
3.3.4 Metabolite characterization of AtST2a and AtSt2b KO lines	67
3.3.4.1 HPLC purification	68
3.3.4.2 Mass spectrometry of purified fractions	69
3.4 Phenotypic analysis of AtST2a and AtSt2b KO lines	75
3.4.1 Effect on germination time	75
3.4.2 Effect on root emergence	77
3.4.3 Effect of different growth media on root length	78
3.4.4 Effect of different photoperiod conditions on root growth	79

3.4.5 Morphological studies	81
3.4.6 Effect on Flowering Time	85
3.4.6.1 Long Day Analysis	86
3.4.6.2 Short Day Analysis	86
3.4.7 Seed production	87
4.0 Discussion	89
4.1 12-OHJA has a biological role, independent of MeJA	91
4.2 Expression of JA- biosynthesis genes in <i>AtST2a</i> - and <i>AtSt2b</i> -KO plants	94
4.3 The function of <i>AtST2a</i> is to sulfonate 12-OHJA and is disrupted in the <i>AtST2a</i> -KO mutant	95
4.4 Decreased internal levels of 12-OHJASO ₄ do not give rise to a visible phenotype in the <i>AtST2a</i> -KO line	97
5.0 Concluding Remarks and Future Work	102
References	104
Appendix	available on CD accompanying this thesis

List of Figures

Figure 1: Shoot apical meristem representation and electron microscope image....	4
Figure 2: Flower development pathways.....	7
Figure 3: Signaling Pathways Involved in the Regulation of Flowering by Photoperiod in <i>A. thaliana</i>	9
Figure 4: Genetic model for floral induction and morphogenesis in <i>A. thaliana</i>	14
Figure 5: Biochemical structure of JA, MeJA and 12-OHJA	16
Figure 6: Scheme of JA biosynthesis and further 13-LOX products derived from α - LeA, 13-HPOT and (9Z,11E,15Z)-13-keto-(9,11,15)-octadecatrienoic acid (13-KOT).....	23
Figure 7: Schematic representation of the metabolic conversions of jasmonates in tobacco BY-2 cells.....	26
Figure 8: Cluster analysis of differentially expressed genes in <i>A. thaliana</i> control, 4h JAME or 4h 12-OH-JA treatments.....	46
Figure 9: RT-PCR validation of microarray experiment in Col0 ecotype for control and plants treated with 50 μ M MeJA or 100 μ M 12-OHJA for 4 hours.....	57
Figure 10: Classification of A) 365 MeJA up-regulated and B) 411 MeJA down- regulated genes into functional groups based on their known, predicted and/or putative biological function.	59
Figure 11: Classification of A) 45 12-OHJA up-regulated and B) 7 12-OHJA down- regulated genes into functional groups based on their known, predicted and/or putative biological function.	60

Figure 12: Classification of A) 145 up-regulated and B) 120 down-regulated genes in response to both MeJA and 12-OHJA treatments into functional groups based on their known, predicted and/or putative biological function.	61
Figure 13: Patterns of <i>AtST2a</i> and <i>AtST2b</i> gene expression in different flowering time mutants and their wildtype background.....	62
Figure 14: PCR determination of homozygous <i>AtST2a</i> and <i>AtST2b</i> mutant lines....	66
Figure 15: RT-PCR results of gene expression patterns of photoperiod (<i>PorA</i>) and jasmonate pathway (<i>AOS</i> , <i>AOC4</i> and <i>OPR3</i>) genes in wildtype, <i>coi1-16</i> , <i>AtST2a-KO</i> and <i>AtST2b-KO</i> ecotypes.	67
Figure 16: HPLC elution profile of 12-OHJA- ³⁵ SO ₄	68
Figure 17: Neutral loss spectrum of wildtype and KO mutants showing presence or lack of 12-OHJA-SO ₄ (mw 305).....	70
Figure 18: Fragmentation patterns of the 305 and 307 ions by MS/MS spectrometry.....	72
Figure 19: Exact mass of 12-OHJA-SO ₄ and broken down fragments in negative mode.....	73
Figure 20: Mass spectra of <i>AtSt2a</i> and <i>AtST2b</i> overexpressing and antisense lines and their respective wildtype control, in negative mode	74
Figure 21: Graphical representation of the germination percentile of the wildtype ecotype <i>Columbia 0</i> , as well as the <i>AtST2a</i> - and <i>AtST2b</i> - KOs and the JA-insensitive <i>coi1-16</i> mutant on MS medium and MS media containing various concentrations of MeJA.	76

Figure 22: Percentage of plants with visible roots on day 3 (germination day) in wildtype and mutants on MS media as compared to MS +100µM MeJA.	77
Figure 23: A) Seeds and B) 2 days old (dark-treated) seedlings of 1) GUS- <i>AtST2a</i> promoter transgenic plants, 2) Col0, 3) <i>AtST2a</i> –KO and 4) <i>AtST2b</i> -KO.....	81
Figure 24: Twelve days old seedlings in A) GUS- <i>AtST2a</i> promoter transgenic c plants, B) Col0, C) <i>AtST2a</i> –KO and D) <i>AtST2b</i> - KO dark-treated for 48h	82
Figure 25: Mature A) apical meristem, B) leaves, C) flowers and D) siliques of 1) GUS- <i>AtST2a</i> promoter transgenic plants, 2) Col0, 3) <i>AtST2a</i> –KO and 4) <i>AtST2b</i> - KO.....	84

List of Tables:

Table 1: Oligonucleotide used for homozygous confirmation	39
Table 2: Oligonucleotide used for gene expression analysis of KOs	40
Table 3: Top 20 genes induced exclusively by MeJA	47
Table 4: Top 20 genes repressed exclusively by MeJA.....	48
Table 5: Top 20 genes induced exclusively by 12-OHJA	49
Table 6: Seven genes repressed exclusively by 12-OHJA	50
Table 7: Top 20 genes induced by both MeJA and 12-OHJA	51
Table 8: Top 20 genes repressed by both MeJA and 12-OHJA	52
Table 9: Comparison of experimental values to known MeJA-induced genes ..	53
Table 10: Comparison of experimental values to known MeJA- repressed groups of genes	55
Table 11: Affymetrix array expression values.....	57
Table 12: Knockout plants grown in soil, independently of photoperiod, germinate at the same time as the wildtype control.....	75
Table 13: Percent germination assessed on day 3 on MS medium, or MS media supplied with 25, 50 or 100 μ M MeJA (n=12)	76
Table 14: Percent of plants showing visible roots on day 3.	77
Table 15: Root length measurements of ten days old <i>coi1-16</i> , <i>AtST2a-KO</i> , <i>AtST2b-KO</i> and their wildtype background, Col0 on MS media, or media supplied with 100 μ M MeJA or 100 μ M 12-OHJA.....	78

Table 16: Root length measurements under different photoperiods of 7 days old coi1-16 <i>AtST2a-KO</i> and <i>AtST2b-KO</i> plants as compared to Col0.....	80
Table 17: Number of days to the first flower and total leaf number for Col0, <i>AtST2a- KO</i> and <i>AtST2b- KO</i> under long day conditions.....	86
Table 18: Number of days to the first flower and total leaf number for Col0, <i>AtST2A KO</i> and <i>AtST2B KO</i> under short day conditions.....	87
Table 19: Seed production in terms of number of seeds per silique of mature (45 days old) plants.	88

List of abbreviations:

12-OHJA: 12-hydroxyjasmonate
13-HPOT: 13-hydroperoxy- octadecatrienoic acid
13-KOT: 13-keto-octadecatrienoic acid
AOC: Allene oxide cyclase
AOS: Allene oxide synthase
AP1: Apetala1
CAL: Cauliflower
CaMV: Cauliflower Mozaic Virus
CO: Constans
Col0: Columbia 0
EMF: Embryonic flower
FLC: Flowering locus C
FMI: Floral meristem identity
FRI: Frigida
FT: Flowering locus T
GA: Giberillic acid
GAI: Giberillic acid insensitive
HPLC: High pressure liquid chromatography
JA: Jasmonic acid
JIMT: JA-induced methyltransferase
LA: Linolenic acid
LD: Long Day (16h light, 8h dark)
Ler: Landsberg erecta
LFY : LEAFY
LOX: Lipoxygenase
MeJA: Methyljasmonate
MS: Murashige and Skoog
OPDA: 12-oxo-phytodienoic acid
OPR: OPDA reductase
PAPS: 3'-phosphoadenosine 5'-phosphosulphate
RMA: Robust Multiarray Analysis
RT-PCR: Reverse transcription-polymerase chain reaction
SAM: Shoot apical meristem
SD: Short Day (8h light, 16h dark)
SOC: Suppressor of overexpression of CO
SOM: Self-organizing maps
SULT: Sulfotransferase
TFL: Terminal flower
UFO: Unusual floral organs
VRN: Vernalization
VSP: Vegetative Storage Protein

1.0 Introduction

Not only source of great joy, purely for their often majestic beauty, plants are much more than this for many species, including our own: they are a source of food, and thus, a source of life. Their importance in our everyday life ranges quite a lot, from necessity in areas where they provide the sole or main part of the diet (cereals), to flowers wilting on our loved one's graves, purely for our hedonistic delight, passing through a diversity of commodities, such as furniture, adornments and drugs. In a world where "natural" is the new trend, even pharmaceutical companies are slowly changing their approach to drug design and are developing a growing interest in medicinal plants as a new source of income. As a consequence of this huge economical impact, a lot of money has and continues to be put into plant research, but their complexities are so puzzling that a great deal still remains to be uncovered.

Many factors limit plant growth in certain geographic areas, and yet more restrain even the usable areas to only several months a year. Furthermore, with a growing population in a restricted environment, the hunger rates are rising every year, even in our own hometowns. We will soon have no choice but to re-evaluate our dependency on the land in a different way that might have to eliminate, or at least drastically reduce our use of it for sustaining meats to provide to a minority of the population, and use it instead to grow crops that could feed the entire population. What we, as researchers, can do, while waiting for the masses to understand the need to change, is work at our own achievable goals: improving the use of land, by manipulating plants to better adapt to extreme

weather conditions (eg. cold, drought or dry) and so expand production to uncultivated areas, or, ameliorating crop production, either by increasing productivity or genetically improving the nutritional content of the crops.

But in order to achieve this, first we need to understand and piece together all the intricate mechanisms that dictate plant development in the wildtype. Only then can we apply this knowledge to accelerate evolution for what suits our needs as a species. The current thesis deals only with the research level, more precisely so with the understanding of a class of plant hormones, called jasmonates, their role in photoperiod perception and flower development. The implications of understanding these processes can then be applied to any of the previously discussed levels, in a continuous process of discovery and advancement.

1.1. Plant life and Flowering: An Introduction

The life cycle of flowering plants can generally be divided into four growth phases: vegetative, reproductive, senescence and dormancy (Poethig 1990). As senescence is the process that occurs near the end of a plant's active life, and dormancy is a state of suspension of physiological activity, we can say that the two major phases in plant life are the vegetative and reproductive ones. Two groups of continually dividing, meristematic cells give rise to all of the structures of the adult flowering plant: the shoot apical meristem (SAM) and the root meristem. These cells are laid down in the developing embryo and form the source for all postembryonic plant organs (Campbell and Reece, 1999). Thus, unlike what is seen in animal morphogenesis, plants retain throughout their lives the ability to continually develop due to these groups of dividing undifferentiated cells.

In the beginning of the vegetative phase, the SAM (figure 1) generates leaves, or the energy harvesting organs. Upon receiving the appropriate environmental and developmental signals, the plant switches to floral or reproductive growth, and the SAM enters the inflorescence phase (I_1), giving rise to an inflorescence with flower primordia (Weberling, 1989). During this phase, the fate of the SAM and the secondary shoots that arise in the axils of the leaves is determined by a set of meristem identity genes, some of which prevent and some of which promote the development of floral meristems (Weberling, 1989).

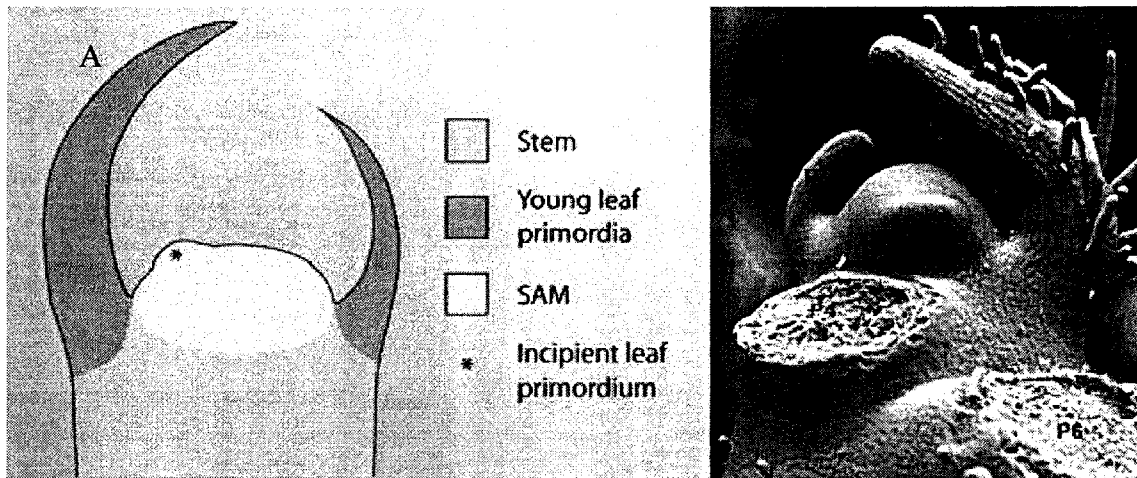


Figure 1: Shoot apical meristem representation (a) (available online at http://users.ox.ac.uk/~sann2453/research_images/SAM.jpg) **and electron microscope image (b)** (available online at <http://www.botany.unibe.ch/deve/research/projects/leafdeve.php>).

1.2. The Switch to Flowering

Flowering plays a primordial role in plant development and survival, as it is what ensures reproductive success. In higher plants, flowering involves the transition from the vegetative phase (generating the leaves and stem) to a reproductive phase (giving rise to the flowers and fruits). The timing and transition to flowering is determined by the interaction of an intricate number of endogenous pathways and exogenous environmental cues that together signal the plant the most appropriate time to flower. All of these efforts are orchestrated in order to increase the chances of successful reproduction. The flowering pathway has been most extensively studied in the model plant organism *A. thaliana*. *A. thaliana* is an obvious choice of study in plant biology due to its many advantages: small size, rapid generation time, fecundity and ability to self-

fertilize, small and fully sequenced genome since 2000 by the *A. thaliana* Genome Initiative (AGI, 2000) and ease of mutagenesis being only few of such examples. Furthermore, the flowering behaviour of *A. thaliana*, as many other processes at both phenotypic and genotypic levels, mimics that of many other plants, making it an excellent organism for plant studies.

1.3 Early and late flowering mutants

A lot of the knowledge available to us so far comes from reverse genetic studies on plant mutants. Indeed, another incentive of working with *A. thaliana* is the great availability, both in wild life and through induced mutagenesis, of mutants in genes spanning over 30% of its genome (The *A. thaliana* Biological Resource Center- ABRC). By looking at mutants affected in their flowering time, scientists have been able to identify many of the transcriptional factors involved in the elaborate process of flowering, enabling us to have a slight idea of how different paths and stimuli interact. Through the study of such mutants, researchers have isolated a number of genes thought to sequentially act to influence flowering. These genes could be grouped into three classes. The first class comprises genes collectively known as **flowering time genes**, which sense the factors to prepare for the switch of the meristem. In the second one, we find the **floral meristem identity genes** that make the actual switch of the apical meristem to reproductive phase. Finally, the last class includes genes that direct the formation of flower, i.e. **the flower organ identity genes** (Levy and Dean, 1998).

1.4 Flowering Time Genes

An extensive number of genes (>80) have been identified to participate in the switch to flowering (reviewed by Simpson *et al.*, 1999). Regulation of these genes was shown to occur through a network of four genetic pathways, where three of them mediate responses to environmental cues: photoperiodic promotion under long days, gibberelin dependent pathway under short days and vernalization, where flowering is promoted in response to a period of seeds' exposure to cold (Levy and Dean, 1998). The other two function independently of such signals: the autonomous pathway promotes flowering under all conditions, and the repression pathway comprises genes that repress initiation of flowering.

1.4.1 The photoperiod pathway

The photoperiod pathway is one of the most important factors controlling flowering time in temperate regions. *A. thaliana* is a facultative long-day plant, which flowers earlier under long days but eventually flowers even under short days. Molecular-genetic approaches have identified genes required for the daylength response. Some of these encode regulatory proteins specifically involved in the regulation of flowering, while others encode components of light signal transduction pathways or are involved in circadian clock function. An overview of the complexity of the interactions of the genes responding to photoperiod can be seen in figure 3 and is extensively reviewed in Blazquez *et al.*, 2000. Only few key factors will be discussed for the purpose of this thesis.

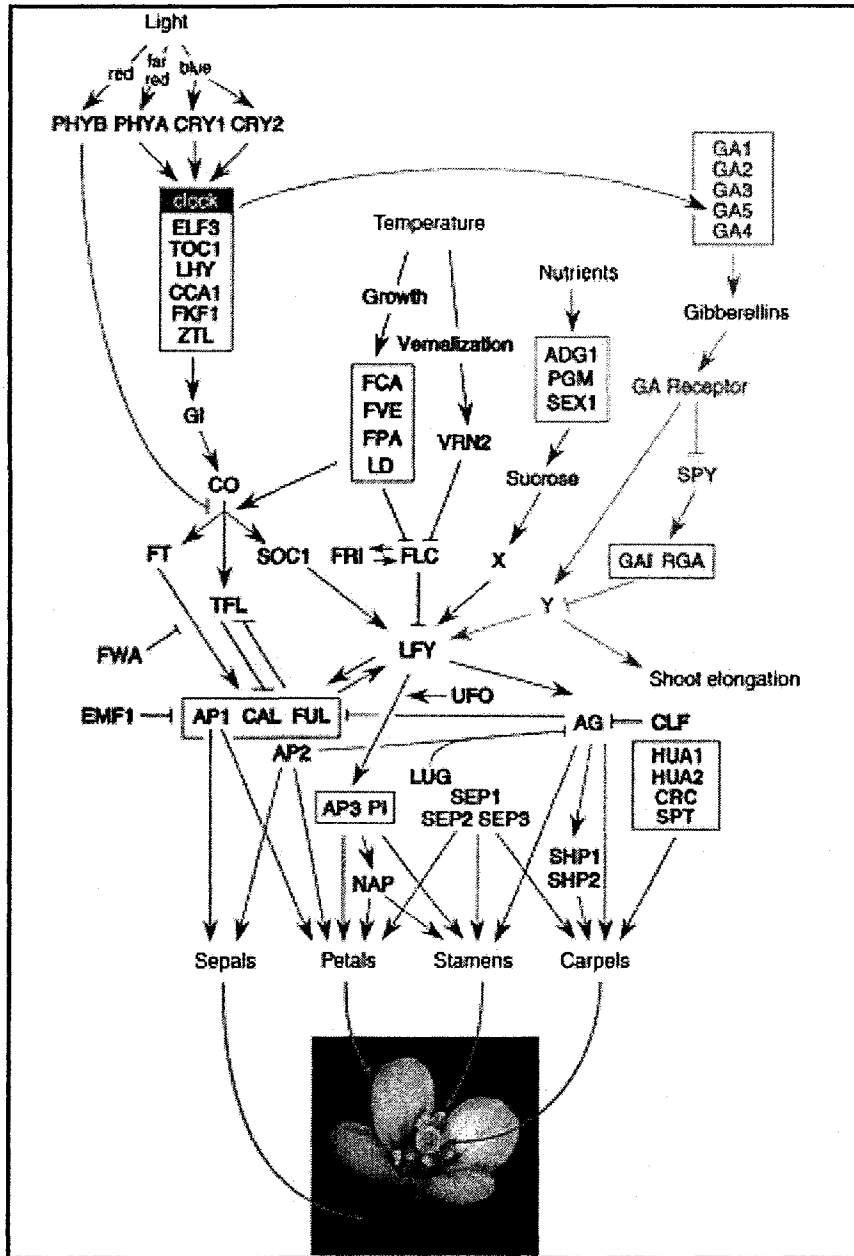


Figure 2: Flower development pathways (from Blazquez, 2000). In red are the photoreceptors and light-activated facultative long-day path. If the photoperiod is short, flowering depends exclusively on a gibberellin-dependent pathway (shown in yellow) and on a photoperiod-independent pathway that is primarily responsive to temperature (shown in blue). In purple are the genes in the nutrient pathway, a reflection of the metabolic state of the plant and thus also flower-promoting. The ultimate targets for the flowering-time pathways are the floral meristem identity genes (shown in green), whose activity confers floral identity to newly emerging primordia. In brown are shown floral meristem identity genes, floral organ identity genes, and mutual interactions between these, which ultimately direct the correct arrangement of floral organs.

1.4.1.1 Long day pathway

The genes involved in the LD pathway comprise the photoreceptors and the circadian clock genes, and directly influence *CONSTANS (CO)* and other genes downstream from it such as *FLOWERING LOCUS T (FT)* and *SUPPRESSOR OF OVEREXPRESSION OF CONSTANS (SOC1)* (see figure 2). *CO* is the most extensively studied of the *A. thaliana* flowering time genes. Inactivation of this gene was shown to cause late flowering, while its overexpression induces early flowering (Putterill et al, 1995; Simon et al, 1996; Onouchi et al, 2000), implying a key role for this gene in the control of flowering time.

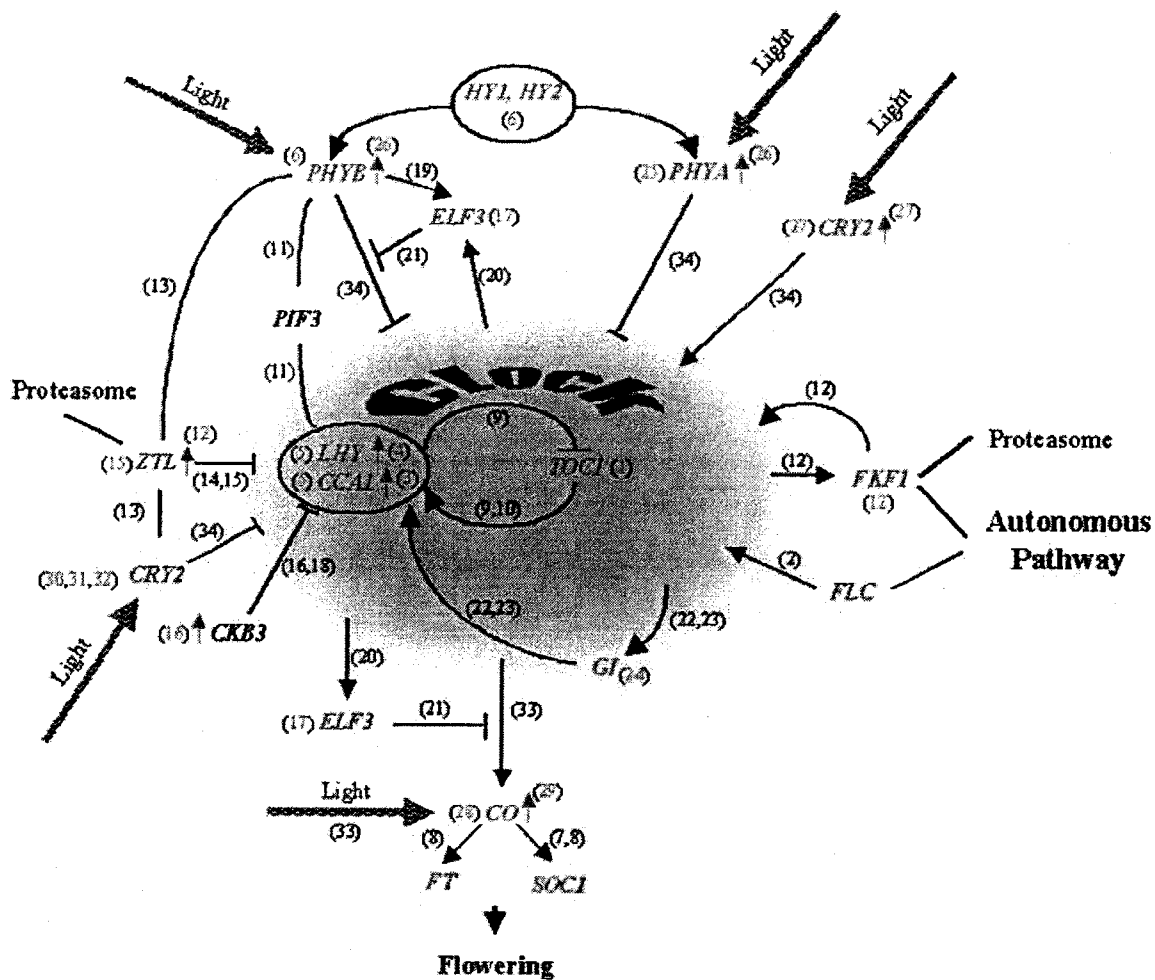


Figure 3: Signaling Pathways Involved in the Regulation of Flowering by Photoperiod in *A. thaliana*. From Mouradov *et al*, 2002. "A diagram showing the putative relationships among genes involved in the photoperiod pathway. On the basis of the phenotypes of known mutants, genes shown in red generally repress flowering, whereas those in green promote it. Small upright arrows indicate the role of the genes as determined by overexpression in transgenic plants. Arrows between genes represent a promotive effect, whereas lines ending with a bar represent a repressive effect, and simple lines represent protein-protein interactions. Arrows from the clock indicate that the expression of the gene is circadian clock controlled. Arrows to the clock indicate that the gene lengthens period length, while perpendicular lines indicate that it shortens period length." The numbers refer to the references in the original publication.

The acceleration of flowering time by long days in *A. thaliana* results in part from the direct effect of light, perceived by cryptochrome 2 and phytochrome A, on the expression of *FT*, a gene that triggers the transition from vegetative to reproductive development when expressed above a certain threshold level. This direct effect of light on *FT* expression requires CO - a Zn-finger transcriptional regulator (Puettrill *et al*, 1995)- whose expression is regulated by the clock such that the overlap between high levels of CO mRNA and the illuminated part of the day is minimal on short days and maximal on long days. So, *FT* mRNA levels accumulate to levels that are sufficient to promote flowering only under the latter condition (Valverde *et al*, 2004). Although the level of FT transcription is extremely sensitive to CO levels and is induced rapidly in response to increasing CO expression, CO is not predicted to bind directly to the FT promoter but probably acts within a protein complex that includes a DNA binding protein that enables attachment of the complex to the FT promoter (Wenkel *et al*, 2006).

CO is also known to act directly on *SOC1*, a MADS-box flowering-time gene regulated by several pathways and proposed to coordinate responses to environmental signals. *SOC1* is directly activated by CO in long photoperiods and is repressed by FLOWERING LOCUS C (FLC), a component of the vernalization pathway (Hepworth *et al*, 2002).

1.4.1.2 Short day pathway (Gibberellin pathway)

The gibberellic acid (GA) pathway is thought to be a signalling path essential for flowering under SD conditions. This is based on the fact that the GA biosynthetic *ga1* mutant of *A. thaliana* never flowers under such conditions (Wilson *et al*, 1992). The phenotype could be rescued with exogenous application of GA. A *gibberellin acid insensitive (gai)* mutant fails to respond to GA treatment and flowers later than wildtype in SD, but does flower (Wilson *et al*, 1992). The fact that a loss of function mutation in GA signalling (*gai*) could rescue the *ga1* phenotype, leads to the conclusion that the GA signal (not the molecule) provides the information for the up-regulation of the SD flowering pathway (Wilson *et al*, 1992).

1.4.2 Autonomous pathway

Mutations that delay flowering under any photoperiod and still responds to vernalization (the requirement of a period of low winter temperature to initiate or accelerate the flowering process) were placed in the autonomous pathway. The autonomous pathway comprises a combination of factors involved in RNA processing and epigenetic regulation that downregulate the floral repressor, *FLC* (figures 2 and 3). The autonomous pathway includes many genes, mutations in each of which lead to an increase in the levels of *FLC* mRNA and FLC protein (Michaels and Amasino, 1999; Sheldon *et al*, 1999; Rouse *et al.*, 2002). Most of the genes in this group have been cloned and the results suggest that the autonomous pathway represents different biological processes. FCA contains an

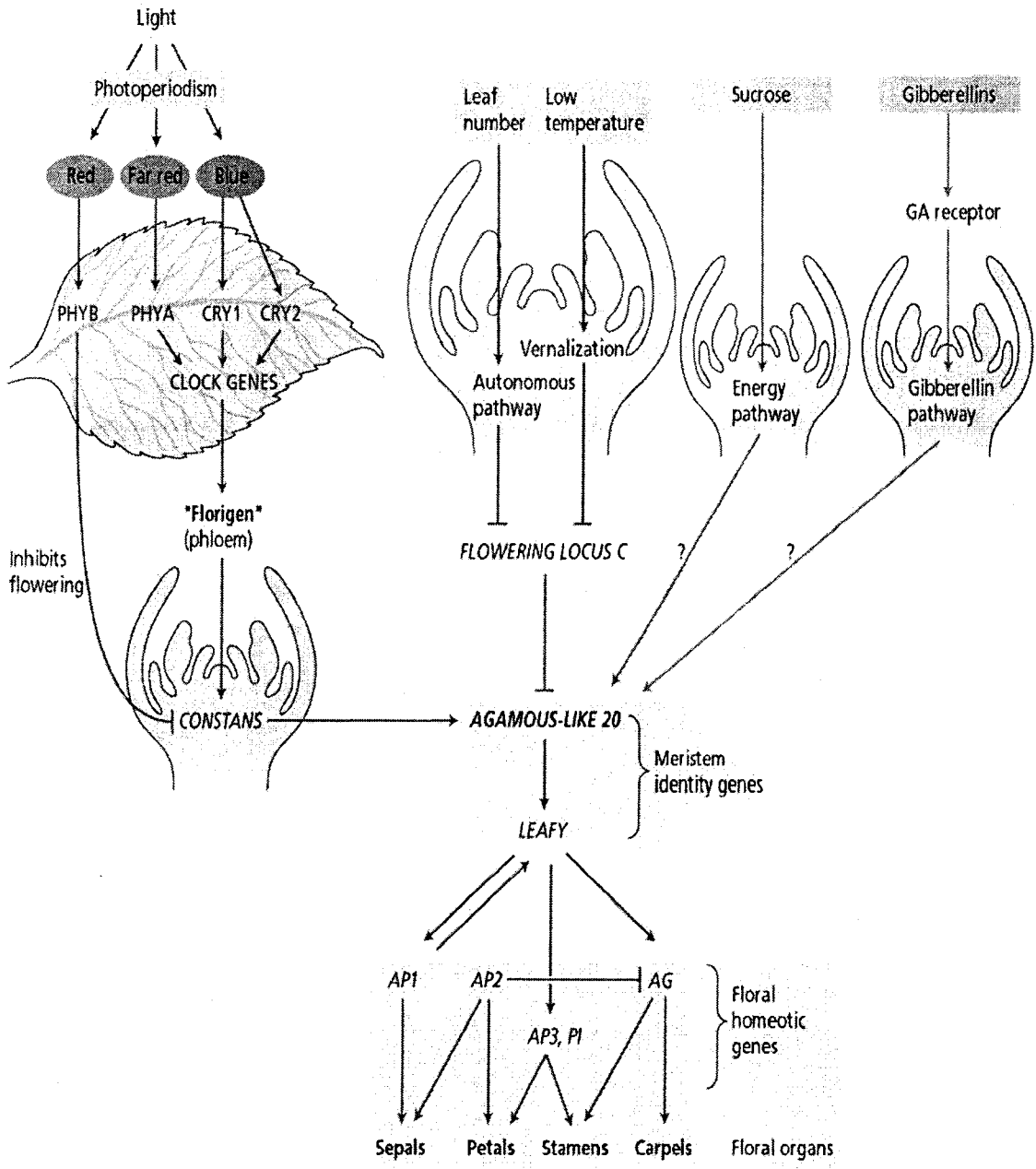
RNA binding motif and a WW domain, which is thought to be involved in protein-protein interactions (Macknight *et al.*, 1997). For example, FCA is able to bind to RNA *in vitro* (Macknight *et al.*, 2002) and regulate its own expression by promoting cleavage and polyadenylation of its own third intron (Quesada *et al.*, 2003). Expression of the *FLC* repressor is mediated by its positive regulator, *FRIGIDA (FRI)*. This coiled-coil domain protein is mutated in early-flowering ecotypes such as Columbia 0 (Col0), Landsberg erecta (Ler) and Wassilewskija (WS), suggesting the gene's wildtype role to induce the flowering repressor *FLC* (Quesada *et al.*, 2003).

1.5 Leaf to Shoot: the 'Florigen' story

We have seen that a variety of factors such as photoperiod, temperature, nutrients and gibberellins coordinate to regulate the floral transition. All of these environmental factors are not perceived by the same plant organs; for example, daylength is perceived by mature leaves and winter cold by the shoot apex (Bernier, 1988). Since flowering occurs in the shoot apical meristem (SAM), floral signals, also called the 'floral stimulus' or 'florigen', are supposed to be produced in response to daylength and translocated from the leaves to the SAM where they induce floral evocation that switches the SAM from leaf production to the initiation of flower buds (see figure 4) (Bernier and Périlleux, 2005; Corbesier and Coupland, 2006).

The physiological study of the floral transition has led to the identification of several putative floral signals such as sucrose, cytokinins, gibberellins, and

reduced N-compounds that are translocated in the phloem sap from leaves to the shoot apical meristem in response to exposure to appropriate day lengths (Corbesier and Coupland, 2006). Grafting experiments have clearly demonstrated that, in response to induction, floral signals are indeed produced in the leaves. For example, in *Perilla*, grafting of a single induced leaf onto an uninduced shoot was sufficient to induce flowering (Zeevaart, 1958). The pattern and velocity of movement of the floral stimulus also appeared to be very similar to that of assimilates, indicating that it is transported through the phloem (King *et al.*, 1968; King and Zeevaart, 1973).



PLANT PHYSIOLOGY, Third Edition, Figure 24.32 © 2002 Sinauer Associates, Inc.

Figure 4: Genetic model for floral induction and morphogenesis in *A. thaliana*.
From Fig 24.32 Taiz & Zeiger.

Although transport of the floral stimulus across graft junctions could be followed indirectly by its effect on flowering, the identity of the stimulus was difficult to establish despite extensive studies that mainly revealed correlations more than direct identification of a causal agent (reviewed in Bernier and Périlleux, 2005; Corbesier and Coupland, 2006). Additional grafting experiments between photoperiod-insensitive plants and photoperiod sensitive plants, or between photoperiod-insensitive plants, gave the same results (i.e. floral induction) (Lang, 1977).

Interestingly, the identified compounds (sucrose, cytokinins, gibberellins, etc) induce in the SAM some of the cellular and molecular events typical of floral evocation (reviewed in Bernier and Périlleux, 2005). However, all these signals do not act, or are not all of equal importance in all species studied. For example, despite GAs being a primary factor in *Lolium temulentum* (King et al., 2001), they are not involved in *Sinapis alba* (Corbesier et al., 2004). This supported a theory known as the “multifactorial control hypothesis” which proposed that several factors, promoters and inhibitors, belonging to the classes of nutrients and hormones, are involved in the control of the SAM floral transition

A similar mechanism is seen in the case of tuberization and the “tuberonic acid” signal that incorporates physical signals to a cascade of internal stimuli. Tuberization in potato plants is controlled by photoperiod and temperature (with short days promoting and long days inhibiting tuberization). It was demonstrated

that the tuberization stimulus is formed in the leaves under short days and is transmitted to the underground parts to induce tuberization.

This “tuberization stimulus” was later shown to comprise 12-hydroxy jasmonic acid glucoside and its methyl ester, known collectively as “tuberonic acid”. This group of four stereoisomers was found to stimulate tuberization in potato and Jerusalem artichoke plants (Koda, 1992). Naturally occurring tuberonic acid is found only in the *cis* conformation and it was shown to exhibit a much stronger activity than the *trans* isomer. The *cis*-tuberonic acid and the glucoside of the tuberonic acid are derived from a known plant hormone, jasmonic acid (figure 5), but in contrast to their precursor, the former have no inhibitory effects on plant growth (Koda, 1992).

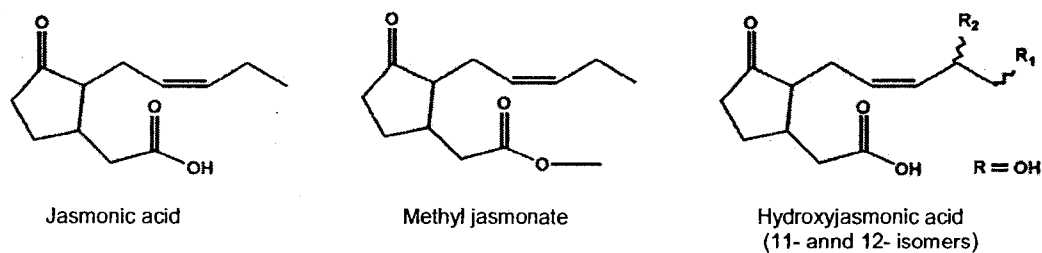


Figure 5: Biochemical structure of JA, MeJA and 12-OHJA

This leads to an interesting question on the more global role of jasmonic acid and its derivative in the context of a network-acting “florigen” signalling and as an integrator of exogenous and endogenous pathways.

1.6 Jasmonic Acid and its Known Roles

1.6.1 Introduction

Jasmonates are signaling molecules that mediate responses to both mechanical trauma and pathogens (Farmer and Ryan, 1992) as well as regulating developmental processes such as germination, flowering time, flower development, fruit ripening and senescence (Van der Fits and Memelink, 2000). Their mode of action seems to be through interactions with receptors in the cells that trigger signalling pathways resulting in transcription, translation and other processes. JA is easily transformed by methylation to its more volatile derivative-MeJA, which has been shown to act as a signal molecule in interplant communication (Weber, 2002). The JA transduction pathway is still largely unknown, due in part to the lipophilic and volatile natures of JA and MeJA, making direct analysis of JA receptors difficult. Many of the responses were monitored under exogenous application of jasmonates, sometimes only confirmed at genetic levels. Interactions between jasmonates and other signalling molecules and regulators make assignment of physiological roles for JA even more complex. Additionally, although most of these responses are observed following plant treatment with MeJA, it is not yet known if MeJA, JA or other derivatives of JA are actually responsible for these phenomena, and it is possible that different roles can be assigned to different components of the jasmonate pathway.

1.6.1.1 Seed Germination and Growth

JA has an opposite role on dormant and non dormant seeds. While it stimulates the germination of dormant seeds (Ranjan and Lewak, 1992), it inhibits that of non-dormant seeds (Corbineau *et al.*,1988; Daletskaya and Sembdner, 1989). The latter (usually inhibited by JA) submitted to dessication increase their concentration of MeJA and JA before the loss of seed viability (Finch-Savage *et al*, 1996). This increase was correlated to lipid peroxidation in the seeds, linking the process of jasmonate production and response to membrane damage rather than germination itself (Finch-Savage *et al*, 1996).

1.6.1.2 Vegetative Storage Proteins and Sinks

Plants are able to accumulate large amounts of carbon and nitrogen in specific cells and tissues, and can mobilize these materials for use in any part of the plant. These abilities are especially useful during seed formation and germination when nutrients need to be concentrated in specific parts of the plant. A role for jasmonates in protein storage comes from their presence in high levels in vegetative sinks. High levels of JA are also present in developing reproductive structures, especially pods, with lower levels in seeds (Koda Y. 1992). Tuberonic acid, a jasmonate derivative, has been proposed to play a role in the formation of tubers, a special type of vegetative sink (Pelacho and Mingo-Castel, 1991).

1.6.1.3 Photosynthesis and Senescence

When JA is applied to plant leaves, expression of nuclear and chloroplast genes involved in photosynthesis is decreased (Weidhase *et al*, 1987). JA treatments also cause loss of chlorophyll from leaves or cell cultures (Weidhase *et al*, 1987), relating this ability to cause chlorosis to the jasmonates' role in plant senescence (Ueda *et al*, 1981). To reconcile this with the fact that JA levels are high in zones of cell division, young leaves and reproductive structures, it has been proposed that JA inhibits the synthesis of chloroplast proteins during an early phase of leaf formation where cell division and import of nutrients are very active (Creelman and Mullet, 1997).

1.6.1.4 Insect and Disease Resistance

Several lines of evidence support JA's role in plant insect and disease resistance. For example, JA accumulates in wounded plants (Creelman *et al*, 1992) and in plants or cell cultures treated with pathogen elicitors (Gundlach *et al*, 1992). JA also induces genes encoding protease inhibitors that help protect plants from insect damage (Johnson *et al*, 1989), as well as genes encoding antifungal proteins such as thionin (Becker and Apel, 1992), osmotin (Xu *et al*, 1994) and PDF (Penninckx *et al*, 1996). Furthermore, the oxylipin pathway that leads to the formation of JA is also the source of other volatile aldehydes and alcohols that function in plant defence and wound healing (Deng *et al*, 1993; Hildebrand *et al*, 1993). Finally, analysis of plants having modified levels of JA also indicates a role for JA in defence and pest resistance. For example,

treatment of potato with JA increases resistance to *Phytophthora infestans* (Cohen *et al*,1993). The tomato mutant JL5, inhibited in the conversion of 13-hydroperoxylinolenic acid to 12-oxophytodienoic acid (OPDA), is more susceptible to damage by *Manduca sexta* (Hove *et al*, 1996).

1.6.1.5 JA in flowering

Jasmonates' role in flower, fruit and seed development was deduced based on their high levels in the reproductive tissues, as well as by the phenotype of JA-deficient mutants. The presence of jasmonates and other related volatile fatty acids is thought to be involved in insect attraction and pollen dispersal, and as thus, a strategy for survival. Combined with JA's role in vegetative storage protein (VSP) induction, as temporary source of carbon and nitrogen, JA ultimately play a role in viable seed formation. This is based on the observation that the JA insensitive mutant *coi1* lacks these VSP proteins and fails to produce viable pollen unless supplied with JA or a precursor in the JA biosynthesis pathway, such as oxophytodenoic acid (OPDA) (McConn and Browse, 1996). The same is true of the JA biosynthesis mutant *12-oxophytodienoate reductase 3 (opr3)*, which lacks the enzyme required to turn the OPDA into the next JA precursor. Exogenously applied JA, but not OPDA, can rescue the male sterile phenotype of this mutant (Stintzi and Browse, 2000)

1.7 JA Biosynthesis

Plants, like animals, are subjected to external and internal stimuli throughout their lives, thus evolution has had to develop multiple ways to respond to these incentives. One path, which bears similarities between the animal and plant kingdoms, is through compounds derived from the oxidative metabolism of polyunsaturated fatty acids. Extensive studies on members of the eicosanoid family of lipid mediators biosynthesized from C20 fatty acids have shown the latter to play a role in regulation of cell differentiation, immune responses and homeostasis in animal systems (Smith *et al*, 2000). In plants, oxygenated derivatives of C18 and C16 fatty acids regulate numerous defense-related and developmental processes (Howe, 2001). Researchers of fatty-acid based signaling in plants have focused upon one hormonally active compound: jasmonic acid (JA) and its derivatives, collectively called jasmonates.

1.7.1 The Jasmonate Pathway

The biosynthesis of JA and its methyl ester was elucidated by Vick and Zimmerman (1983) and Hamberg and Hughes (1988). The main pathway through which JA is synthesized is through the octadecanoid pathway from linolenic acid (LA) (Fig. 9). Synthesis begins with phospholipase A1-release of LA, followed by oxygenation by 13-lipoxygenase (13-LOX) (Ishiuro *et al*, 2001). The resulting 13-hydroperoxide is dehydrated by allene oxide synthase (AOS) to an unstable epoxide (Hamberg and Fahlstadius, 1990), which then reacts readily with allene oxide cyclase (AOC) to form the cyclopentenone ring-containing

OPDA. This compound can further be metabolized by reduction of the ring double bond, reaction catalyzed by OPR3, yielding a cyclopentanone intermediate. Following three rounds of β -oxidation, this intermediate is converted to jasmonic acid, the best-known jasmonate regulator (Creelman and Mullet, 1997). Both OPDA and JA have multiple fates within the plant tissues. They can either be conjugated by esterification to other molecules such as galactolipids in the case of OPDA (Stelmach *et al*, 2001) and various amino acids or simply a methyl group in the case of JA (Creelman and Mullet, 1997).

Mutants that are defective in either the biosynthesis or perception of JA are dramatically compromised in resistance to many plant stresses (Howe *et al*, 1996, McConn *et al*, 1997 and others). These studies have led to the general assumption that JA is the physiological signal for wound and pathogen induced responses. Further studies on an *A. thaliana opr3* mutant, in which OPDA is not transformed into JA, show that these plants also elicit defense response (Stintzi *et al*, 2001), and thus, OPDA is also active as a signal, without prior metabolism to JA. This in turn points to the possible role of other components of the JA pathway as signalling molecules.

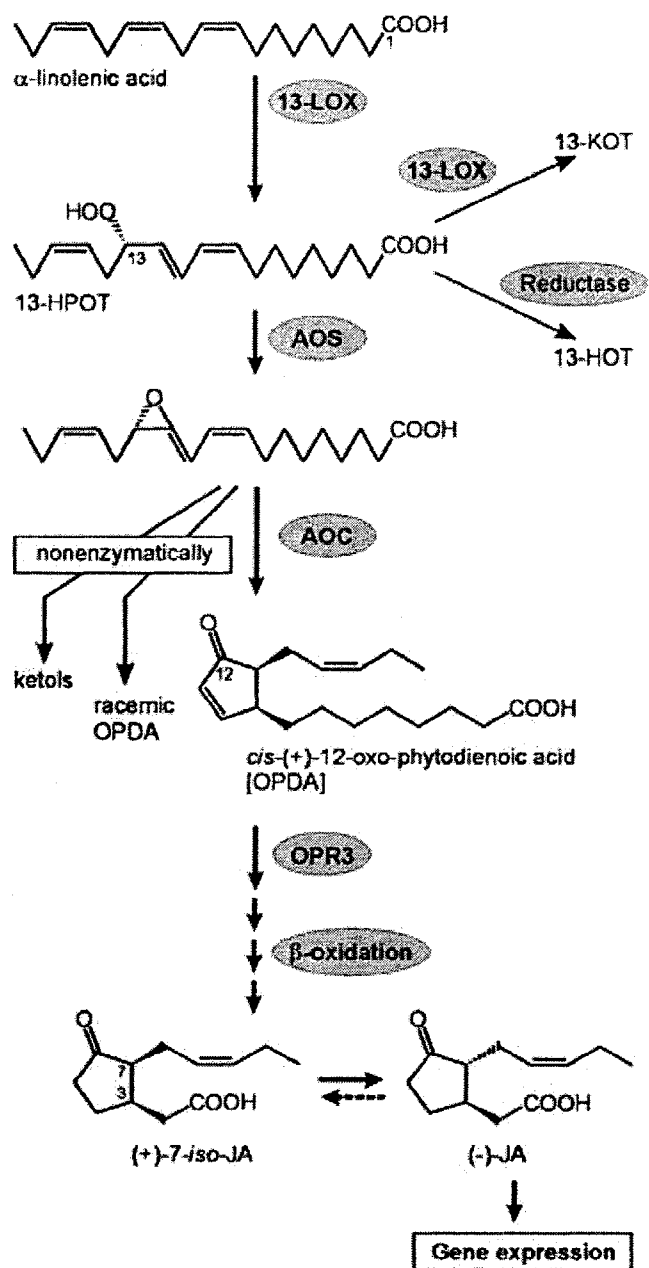


Figure 6: Scheme of JA biosynthesis and further 13-LOX products derived from α -LeA, 13-HPOT and (9Z,11E,15Z)-13-keto-(9,11,15)-octadecatrienoic acid (13-KOT). Identical reactions occur with LA as substrate, whereas the corresponding 9-derivatives are formed via 9-LOX catalysis. From Stenzel *et al*, 2003.

1.7.2 JA metabolites

In fact, although JA biosynthesis is well studied, the metabolic pathways downstream of JA are less understood. The function of particular modifications remains unclear, as there are many contradictory data on the biological activity of JA metabolites. For example, JA, MeJA and 12-OHJA induce tuber formation in potato (*Solanum tuberosum*) (Koda *et al*, 1991), but the latter fails to activate the JA-sensitive element in the promoter of cathepsin D inhibitor, while MeJA is as effective as JA in promoting its activity (Ishikawa *et al*, 1994). 12-OHJA is also inactive in the assay for tendril coiling, a typical response to octadecanoids (Blechert *et al*, 1999). As such, not all the activities associated with JA are shared by its metabolites.

One more example of this exclusivity of response is the JA's ability to arrest tobacco Bright Yellow-2 (BY-2) cells in the G2 phase of the cell cycle (most effectively so when applied 4 hours prior to the G2/M transition) None of its metabolites can elicit the same cell-cycle arrest (Swiatek *et al*, 2004).

Another debated issue was whether MeJA or JA is the active form in inducing jasmonate-specific responses. Studies of a mutant overexpressing the JA-induced methyltransferase (*JIMT*) lead to the conclusion that MeJA is an active compound, independently of its hydrolysis to JA. This was based on the observation that in the *jimt* mutant, the JA responsive genes were induced, as well as the endogenous levels of MeJA, while the JA levels in the plant were unaffected (Seo *et al*, 2001). On the other hand, JA- and MeJA-feeding experiments demonstrate that the latter compound was rapidly hydrolyzed to JA

and further processed as JA (Swiatek *et al*, 2004). Thus, although the effect of MeJA, might be due to its hydrolysis to JA, a direct effect of MeJA cannot be excluded.

A study of the uptake of JA and its metabolism in tobacco (*Nicotiana tabacum*) BY-2 cultures reveals that JA is taken up from the medium and converted into several, more polar, compounds (see figure 7; Swiatek *et al*, 2004).

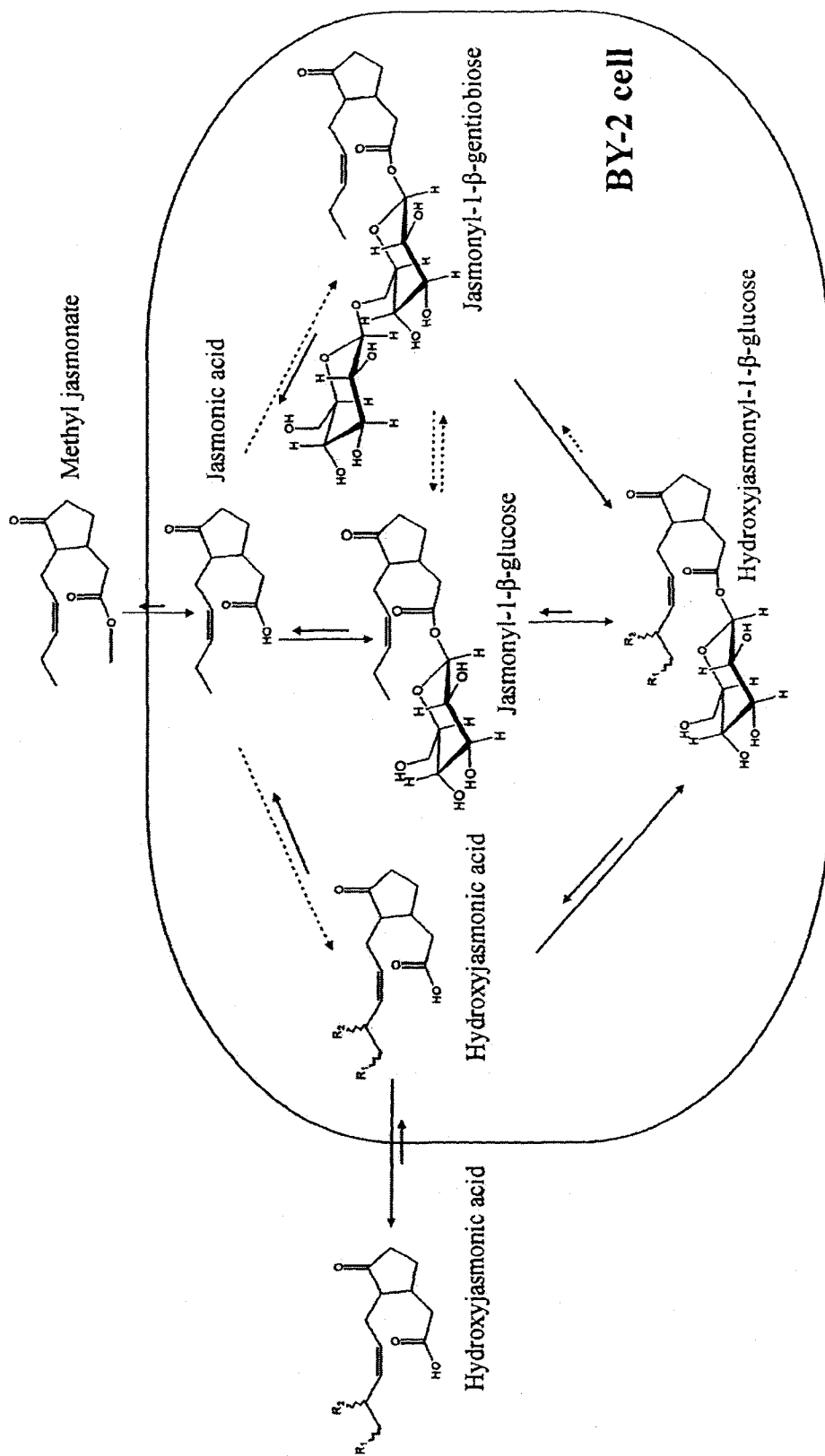


Figure 7: Schematic representation of the metabolic conversions of jasmonates in tobacco BY-2 cells. Reversible steps are marked with opposing arrows. The steps for which insufficient information was available to allow verification are marked with dotted lines. From Swiatek *et al*, 2004.

Among these, free hydroxylated JA was the preferential fraction in the medium of the BY-2 cells treated with different JA metabolites, but not in the cell extracts. This extracellular accumulation makes them a good candidate for long-distance transport and/or removal of superfluous jasmonates. OHJAs have also recently been identified to be a natural constituent in plants as distantly related as potato, *A. thaliana* and barley, indicating the widespread occurrence of hydroxyjasmonates in the plant kingdom (Gidda *et al*, 2003). Its presence in non tuber-forming plants points to other roles for this molecule, outside of its tuber-inducing properties. For example, a hydroxyjasmonate sulfotransferase in *A. thaliana* was shown to be induced by both JA and 12-OHJA (Gidda *et al*, 2003). In conclusion, there seem to be at least two types of jasmonate effects: some, such as tuber formation, are triggered by a family of structurally related compounds, whereas others, such as G2 arrest, look more specific to JA and MeJA, and so might function through a different signal transduction pathway.

1.8 Sulfotransferases and the Sulfonation Reaction

1.8.1 Roles of Sulfonation

Sulfonation is an important reaction in the metabolism of a wide range of xenobiotics, drugs, and endogenous compounds. A supergene family of enzymes called sulfotransferases (SULTs) catalyze this reaction (1st reported by Baumann, 1876). All SULTs use 3'-phosphoadenosine 5'-phosphosulphate (PAPS) as the sulfuryl donor and transfer the sulfonate group to an appropriate hydroxyl group of several classes of substrates (Weinshilboum *et al*, 1997). They have highly conserved domains and can be found in all organisms from eubacteria to eukaryotes (Klein and Papenbrock, 2004). Most of the time, the addition of a sulfonate moiety to a compound increases its water solubility and decreases its biological activity (Klaassen and Boles, 1997). However, many of these enzymes are also capable of bioactivating procarcinogens to reactive electrophiles (Falany, 1997a; Weinshilboum *et al.*, 1997) or can be responsible for the development of hormone-responsive tumours in humans (Duanmu *et al*, 2001).

1.8.2 *A. thaliana* Sulfotransferases

As mentioned before, in mammals SULTs have been shown to be involved in the transformation of xenobiotics, and to modulate the biological activity of hormones and neurotransmitters (Vargas *et al*, 1994; Falany, 1997b; Weinshilboum *et al*, 1997). In plants, these reactions play a role in plant growth, development and adaptation to stress (Klein and Papenbrock, 2004). In total, the *A. thaliana* SULTs family comprises 18 members (based on sequence similarity

of nucleotide and translated products) (Klein and Papenbrock, 2004), of which only few have been fully characterized. All of them have been categorized as cytosolic SULTs, referring to their ability to be extracted from cells in a soluble form. Most of the SULTS have been grouped based on the small organic molecules that they sulfonate.

1.8.3 The *A. thaliana* AtST2 Subgroup and its Regulation

Two of the 18 sulfotransferases, At5g07010 (AtST2a) and At4g07000 (AtST2b) have been grouped in the same subgroup based on their high sequence similarity (85% identity and 92% similarity at the amino acid level). Despite this, genetic analyses have shown that the two enzymes are differentially regulated and are highly selective in their choice of substrate, AtST2b not exhibiting any activity with the substrate of AtST2a (Levitin, A; personal communication). In fact, not much is known about the former. AtST2a has been shown to sulfonate 12-OHJA, with the proposed role of either participating in the inactivation of JA or, as a mean of controlling the biological activity of 12-OHJA (Gidda *et al*, 2003).

1.8.4 12-hydroxyjasmonate as a Signalling Molecule

JA can be transformed by hydroxylation, to result in the 11- or 12-OHJA derivatives. 12-hydroxyjasmonate, also known as tuberonic acid, was first isolated from *Solanum tuberosum* and was shown to have tuber-inducing properties (Yoshihara, *et al.* 1989). Our lab has shown that 12-OHJA occurs

naturally in *A. thaliana*, and has proposed that MeJA and 12-OHJA act through separate pathways. This conclusion has been achieved after treating plants with exogenous 12-OHJA and finding that the expression of the methyljasmonate-responsive gene *Thi2.1*, is not induced (Gidda *et al*, 2003). Furthermore, 12-OHJA has been proposed to act as a signal that promotes the transition from vegetative to reproductive growth when *A. thaliana* is exposed to an inductive photoperiod (Gidda *et al*, 2003).

1.9 Purpose of Current Work

Based on the previous observations of a separate pathway for 12-OHJA, and the study of its sulfonation by the *AtST2a* sulfotransferase, we wanted to further investigate gene regulation by JA and 12-OHJA, and determine if indeed they regulate separate sets of genes, or *Thi 2.1* was just an exception. In order to do this, we performed microarray experiments to compare transcript levels in treated and untreated plants. We also investigated the phenotypes of *AtST2a* and *AtST2b* knockout plants by observing development of tissues or organs known to express *AtST2a* at the highest levels, and monitoring flowering time under SD and LD conditions. The results of these experiments are presented in the current thesis.

2.0 Materials and Methods

2.1. Materials

Columbia 0 (Col0) and *Landsberg erecta (Ler)* wildtype *A. thaliana* seeds and C24 seeds (a near wildtype strain of *A. thaliana* which contains a *FRIGIDA (FRI)* allele that causes late flowering and an *FLC* allele which suppresses the late-flowering phenotype of *FRI*) from Lehle seeds (<http://www.A.thaliana.com>). The CO-2 (*Ler*), *Fca1 (Ler)*, *Fca2 (Ler)* and *Toc1 (C24)* mutant lines were obtained from ABRC (<http://www.biosci.ohio-state.edu/~plantbio/Facilities/abrc/abrchome.htm>). *Coronatine insensitive 1-16 (Coi1-16)* homozygous mutant seeds were kindly donated by Dr. Turner, University of East Anglia, Norwich, England. *AtST2a* (At5g07010) heterozygous T2 knockout seeds (*AtST2a*- KO) line 149G04 were obtained from the GABI-Kat seed collection in Germany. *At2T2b* (At5g07000) heterozygous T2 knockout seeds (*AtST2b*- KO) line SALK_009093.54 were obtained from the SALK T-DNA seed collection (http://www.gabi-kat.de/db/seed_request.php). Both mutants were generated in a Col0 background.

2.2 Methods

2.2.1 Microarray experiment

2.2.1.1 Seed sterilization and Plant growth

A. thaliana (ecotype Columbia-0) seeds were treated for 30s with 70% ethanol, followed by 5 min shaking in a sterilizing mix (10% bleach, 0.02% SDS) and then washed 3 times with sterile dH₂O and placed for 2-4 days at 4°C for stratification (treatment meant to simulate winter conditions). Sterilized seeds were then grown in Magenta boxes on MS media (Murashige and Skoog, 1962) to 16 days of age, under a 16-h light photoperiod. The plants were then treated for four hours with methanol (control), 50µM MeJA or 100µM 12-OH-JA dissolved in methanol, by spraying the solutions on the plates, in the case of the control and 12-OHJA treatment, and placing the appropriate amount on filter paper inside the plates, for the MeJA treatment

2.2.1.2 RNA extraction

The tissue was collected, ground to powder in liquid nitrogen and RNA was extracted by a modification of the phenol-chloroform method (Maliga *et al*, 1995). Each extraction consisted of material from 20-25 plants (representing approximately 3g of fresh tissue). The powder was then transferred to an equal volume of extraction buffer (Tris HCl pH 9.0 0.2M, NaCl 0.4M, MgOAc 0.02M, sucrose 0.5M) to which 1/10 volume of 10% SDS and 1/20 volume of EDTA

400mM has been added. The two components were mixed well and 1 volume of phenol (25): chloroform (24): iAA (1) mixture was added. This was then agitated vigorously without stopping for 20 minutes and centrifuged 15 min at 4000 rpm. The aqueous phase was transferred to a new tube, extracted with equal volume of phenol: CHCl₃: iAA, then shaken again for 20 min, and centrifuged as above. Following the second centrifugation, the aqueous phase was transferred to a new tube, and precipitated with 0.6 volume of isopropanol for 30 min on ice or at 4°C. The RNA was collected by centrifugation at 13 000 rpm for 12 min at 4°C. The aqueous phase was discarded and the pellet re-suspended in DEPC-treated H₂O with 2M LiCl (final concentration) and incubated overnight at 4°C. The next day, the mixture was spun at 9000 rpm for 20 min at 4°C and the pellet re-suspended in DEPC H₂O to which was added 1/10 volume NaOAc 3M (pH5.2) and 2 volumes of 95% ethanol (EtOH). Following a last overnight precipitation at -20°C, the mixture was centrifuged 20 min at 13 000 rpm (4°C), the pellet was washed with 70% EtOH, spun down as above (13 000 rpm) for 5 min, dried and re-suspended in 20 µl DEPC H₂O.

Triplicate extractions from two individual experiments were pooled together to generate the sample used for the microarray hybridization experiment on the *A. thaliana* ATH1 Genome Array (Affymetrix®). Technical replicates were generated as each sample was used for two distinct microarray experiments. The quality and quantity of RNA were confirmed by agarose gel electrophoresis, absorbance 260/280 as well as the Agilent 2100 Bioanalyzer version A.01.16, prior to probe synthesis.

2.2.1.3 Microarray analysis using the *A. thaliana* ATH1

Genome Array

The cRNA synthesis, labeling and chips hybridization were performed as per Affymetrix®'s protocols (McGill University and Genome Quebec Innovation Center). Briefly, this consists of reverse transcription of the target RNA into cDNA, followed by in-vitro transcription as to generate biotin-labeled cRNA. After overnight hybridization, the chips were stained with streptavidin-phycoerythrin and arrays were scanned using a GeneArray Scanner at an excitation wavelength of 488nm. The data was generated by recording the light emission at 570nm, which is proportional to the bound target at each oligonucleotide position on the GeneChip® array. In this study, the Affymetrix® ATH1 Genome Array GeneChip® was used, containing probe sets for approximately 24,000 predicted and known expressed *A. thaliana* genes. The sequences of *E. coli* genes *bioB*, *bioC*, *bioD*, *B. subtilis* gene *lysA* and the phage P1 *cre* gene were used as negative controls, along with the *A. thaliana* maintenance genes GAPDH, Ubiquitin and Actin.

2.2.1.4 Data analysis

The intensities read by the GeneArray Scanner were used as relative expression units and further processed to generate clusters of genes regulated by either one or both of the metabolites. High density oligonucleotide arrays typically use oligonucleotides of around 25 bases and each gene is generally

represented by 11 pairs of oligonucleotides, or probe sets (Irizarry et al, 2003). Of interest to us is to combine the values for these probe pairs to obtain a measure of expression that represents the amount of corresponding mRNA. The analysis process consists of three steps:

Low-level normalization

In order to have confidence in the end result of our analysis, of crucial importance is this first step of normalization. This step allows us to differentiate between “obscuring variation”- due to technical variation such as labeling, hybridization or scanning, and “interesting variation”-that which occurs as a direct effect of the treatment. Many software-based programs have been designed to computerize this step. In Affymetrix chips, each oligonucleotide pair is represented by a *perfect match* (PM) oligonucleotide (i.e. identical to the gene) and a *mismatch* (MM) component, which contains one mutation in the middle (13th) base. The difference in intensities between the two members of a pair allow for non-specific binding measurement. Some software use the difference between the PM and the MM intensities as a measure of normalizing the data, but this has proven obsolete, and newer analysis methods rely on the PM values solely. One such method developed specifically for Affymetrix GeneChips® is the Robust Multichip Average (RMA) analysis. This technique allows probe-specific background correction to compensate for nonspecific binding using PM distribution rather than PM-MM values and multichip quantile normalization to unify PM distributions across all chips in the experiment. Additionally, it provides

robust probe-set summary of log-normalized probe level data by median polishing.

Identification of differentially expressed genes

Once the data had been normalized, we needed to extract only “significantly regulated genes”, and then organize them according to their regulation pattern. This filtering process was performed using the GeneCluster version 2.1.7 (Tamayo et al, 1999) software according to the following parameters: min value= 50; max value= 20,000; max/min= 3 max-min= 100, The normalization step combined with this filtering step allowed us to work only with reproducible probes exhibiting ≥ 2 -fold difference in average between the MeJA- or 12-OHJA-treated, and the mock-treated plants.

Clustering Analysis and Functional Interpretation

Finally, these genes were clustered with the software’s self organizing maps (SOMs) function into related subsets based on a distance metric across elements. Basically, this allows easy visualization of similarly expressed patterns. The genes were the organized into 2 SOM rows, 4 SOM columns (resulting in 8 clusters). Except for the rows and columns specifications, the basic and advanced parameters were left as standardized by the program. The clusters were then organized by their biological process using the Data Mining Tool available from the Affymetrix Netaffx Analysis center (<http://www.affymetrix.com/>

[analysis/index.affx](#)) and manual functional assignment into categories based on their biological function.

2.2.2 Reverse-Transcription PCR

Plants (ecotype *Col0* and *coi1-16*) were grown and treated as previously described, and the RNA was used to synthesize the cDNA template for PCR validation of the microarray experiment. Two μg of RNA prepared as above (2 to 17.8 μL , depending on the concentration of RNA) were added to 2 μL Expand Reverse Transcriptase (RT) Buffer 5x (Roche Applied Science) and 0.2 μL RNase free DNaseI 40U/ μL (Roche Applied Science). The volume was adjusted to 20 μL using DEPC-treated water. The reaction was incubated 15 min at room temperature, and then 2 μL 30mM EDTA was added. After another incubation of 10 minutes at 65°C to inactivate the DNase, the tubes were put on ice for 2 min and centrifuged briefly. Following the DNase treatment, 8 μL of 50 μM Oligo dT (15mers) was added to each of the reactions and the tubes were incubated 10 min, at 65°C, then put on ice for 2 min and centrifuged briefly. A mix of 10 μL Expand RT Buffer 5x, 5 μL dTT (100mM), 2 μL dNTP (25 mM), 1.25 μL RNase inhibitor 40U/ μL and 2.5 μL Expand RT (for positive RT reactions) 50U/ μL (all from Roche Applied Science) was added to each reaction, followed by a 60min incubation at 43°C. The cDNA was then used in several polymerase chain reactions (PCRs) to validate the results of the microarray experiment. The internal control Actin4 gene, as well as a pair of universal primers for 8 of the

actin genes were used to equalize the quantity of cDNA of the different samples and selected genes were tested to confirm the gene expression pattern observed in the microarray experiment.

2.2.3 Phenotype analysis

2.2.3.1 Plant growth conditions

Plants were grown in soil (Fafard Agromix #2) in environmental *A. thaliana* growth chambers (Conviron S15) under a light intensity of $50\mu\text{M m}^{-1} \text{s}^{-1}$. For the long day (LD) conditions, 16h of light and 8h of dark were provided in order to mimic summer time conditions. For the short day (SD) conditions, 8h of light and 16h of dark were provided, to simulate wintertime conditions. In both cases temperature was kept at 22°C in the night time period, rising gradually in the last hour of dark to reach 24°C during the daytime period. Plants were provided with a solution of 4g/l 15-30-15 N-P-K fertilizer every two weeks to ensure proper nutrients delivery at all times. The day of the first flower and the total leaf number was recorded for 32 plants from each genotype, both under LD and SD.

2.2.3.2 Genomic DNA extraction

One leaf from each, Col0, *AtST2a*-KO plants 1-24 and *AtST2b*-KO plants 25-48 was collected, ground in liquid nitrogen and resuspended in 2X CTAB buffer. The mixture was incubated at 65°C for 40 min with vortexing once after 20 min. The aqueous phase was then extracted with equal volume of phenol-

chloroform (1:1), followed by chloroform and then precipitated overnight with 1/10 volume NaOAc 3M pH 5.2 and 0.6 volume isopropanol at -20°C. The next day, a 70% EtOH wash was performed and the genomic DNA (gDNA) was resuspended in water.

2.2.3.3 Confirmation of Homozygous Mutant

Polymerase chain reaction was performed on 50ng gDNA from each of the three samples using the following gene primers:

Table 1: Oligonucleotide sequences used for homozygous confirmation

Gene	Sequence
Actin 2 (At3g18780)	F 5' GCTGATGGTGAAGACATTCA 3'
	R 5' CATAGCAGGGGCATTGAAAG 3'
AtST2a (At5g07010)	F 5' GGAGAGAGGATGGAGAAC 3'
	R 5' ATCCACTAAGGCTGACAATC 3'
T-DNA LB	F 5' CATTGGACGTGAATGTAGA 3'
AtST2b (At5g07000)	F 5' TTGACACATTCATCTCCATG 3'
	R 5' CATTAGCTACATACATACATGCATGA 3'
T-DNA	R 5' CAAACAGGATTTTCGCCT 3'

2.2.3.4 Methyljasmonate and 12-Hydroxyjasmonate

Treatments

Sterilized seeds were grown vertically on Murashige-Skoog medium with 0.1% ethanol (control), 100uM MeJA and 100uM 12-OHJA (dissolved in 0.1% EtOH) in large (15cm diameter) petri dishes. Root length analysis and germination rates were determined for wildtype, *coi1-16*, *AtST2-a KO* and *AtST2b- KO* plants.

2.2.4 Gene Expression Analysis of *AtST2a* and *AtST2b* KOs

PCR was performed on cDNA samples from *Col0*, *coi1-16*, *AtST2a- KO* and *AtST2b- KO* plants grown under LD conditions (control) or exposed to dark for 48 h. The following primers were used for amplification:

Table 2: Oligonucleotide sequences for gene expression analysis of KOs

Gene	Sequence
PORA (At5g54190)	F: 5'ATTTGGACTTGGCGTCTTTG3'
	R: 5' AGGGAAGAGGGTACGGAAAA3'
AOS (AT5G42650)	F: 5'GTCAGAACTCCTGATCTAACCG 3'
	R: 5'GGTACGAGAGGATACGGTAGC 3'
AOC4 (AT1G13280)	F: 5'AGGAACCTCTCTCGCAATCA3'
	R: 5'GAAGCTTCAAAGCGATCACC3'
OPR3 (AT2G06050)	F: 5'CCAATACGGAGGATCCATTG3'
	R: 5'GGGAAAAAGGAGCCAAGAAA3'

2.2.5 Mass Spectrometry

A. thaliana ecotype Col0, *AtST2a*-KO and *AtST2b*-KO seeds were planted on MS Petri dishes and grown to 16 days of age. Prior to extraction, plants were treated for 48 h with 100 μ M MeJA to ensure sufficient levels of 12-OHJA sulfate detection (in wildtype). On the day of extraction, approximately one gram of tissue was ground to a fine powder in liquid nitrogen and homogenized in 50% methanol (ca 5 ml per gram tissue). The homogenate was centrifuged at 10,000 RPM for 5 minutes to remove the cellular debris. The methanol was removed from the clarified extract by evaporation under reduced pressure. The remaining aqueous solution was extracted with one volume of butanol and the butanolic fraction containing the jasmonate derivatives was lyophilized using a SpeedVac concentrator. The lyophilized samples were resuspended in 100 μ l of 50% methanol for HPLC purification

2.2.5.1 HPLC Fractionation of Wildtype, *AtST2a*- KO and *AtST2b*- KO Extracts

The 50% methanolic extracts (c.a. 100 μ l) were fractionated by reverse phase chromatography on a NovaPack C₁₈ column (Waters, USA). The separations were performed on a Waters 625 HPLC system using the following gradient:

0 – 10 minutes isocratic 100% A

10-50 minutes from 0 to 70% B

50-60 minutes from 70% to 100% B

Flow rate 0.5 ml per minute, fraction size 1 minute.

Solvent A = water containing 0.05% acetic acid and 5 mM ammonium acetate

Solvent B = methanol containing 0.05% acetic acid

The retention time of 12-OHJA sulfate was determined by the injection on the C₁₈ column of the reaction product catalyzed by AtST2a with an authentic sample of 12-OHJA in presence of [³⁵S]-labeled PAPS. 200 µl of each fraction was mixed with 3 ml of scintillation fluid and counted for radioactivity on a liquid scintillation counter.

2.2.5.2 Neutral loss mass spectrometry of purified metabolites from wildtype, *AtST2a* and *AtST2b* extracts.

The HPLC-purified fractions were analysed using neutral loss ESI-mass spectrometry in the negative mode in search of a parent ion with a molecular mass at 305 (M-1) which gave a neutral loss of 80 mass unit. The analysis was performed on a Quattro triple quadrupole mass spectrometer (Micromass, UK) using a cone voltage of 20V and a collision energy of 35V. The spectra were acquired with a duration of 2 seconds and an interscan delay of 0.1 second. In

order to validate the structure of the compounds identified by neutral loss mass spectrometry, the same extracts were analyzed by ESI-MS/MS on a Q-ToF 2 spectrometer in the negative mode (Micromass, UK). The samples were processed using a cone voltage of 10V and collision energy of 35V. The spectra were acquired using the Masslink software form Micromass.

3.0 Results

3.1 Effect of MeJA and 12-OHJA on Gene Expression

3.1.1 Introduction

Previous experiments have shown that MeJA and 12-OHJA do not elicit the same morphological responses in plants (Gidda *et al*, 2003, Levitin, 2004), and that genes might be differentially regulated by the two metabolites (Gidda *et al*, 2003). The data support the possibility of a separate role for these metabolites in plant growth. Our objective was to test this hypothesis in order to better understand the biological function of the two metabolites, by looking for genes, if any, which are regulated exclusively by one of the two compounds, versus those which behave similarly. This, in turn, would indicate the presence of separate regulatory pathways responding to the two metabolites. The obvious choice to perform such an experiment was the use of microarray, in our case the Affymetrix® ATH1 full genome array. This method was justified by the genome-wide effects that can be monitored, and was used to investigate gene regulation after 4h MeJA or 12-OHJA treatments, as compared to the 4h mock-treatment on wildtype *A. thaliana* (Columbia 0). A relatively short time point was selected based on previous information that this was enough to induce marker genes such as *Thi2.1*, as well as genes in the JA biosynthetic pathway (Gidda *et al*, 2003, Levitin, 2004). Furthermore, MeJA is known to regulate a series of transcriptional cascades which impact on later developmental and physiological changes, biasing the data after longer time treatments. The plants were grown to 16 days

of age, before the dramatic change in the internal level of jasmonates associated with flowering.

3.1.2 Microarray Analysis

Following data analysis (see Materials and Methods), 1763 genes (7.75% of the total number of genes) showed a significant increase or decrease in expression of at least two fold following one of the treatments, as compared to the control and are referred to as “significantly regulated genes”.

The genes were organized into clusters with the main goal to detect sets of genes regulated differently by the two metabolites (Tables 3-8). Cluster analysis results are summarized in Figure 8.

In total, 376 genes were induced exclusively by MeJa (cluster 0), while 412 genes were inhibited exclusively by MeJA (cluster 7). Only 45 genes were found to be exclusively induced by 12-OHJA (cluster 6) and 7 genes were repressed solely by the latter compound (cluster 1). Finally, 152 genes were induced (cluster 5) and 134 genes were repressed (cluster 2) following treatment with both compounds.

The twenty genes in each cluster that were induced or repressed by the greatest amount are presented in Tables 3 to 8. The full list of genes included in the analysis can be found in Annex 1. Tables 9 and 10 compare known regulated genes (Zimmermann *et al*, 2004) to our own results, for added confidence in the microarray results.

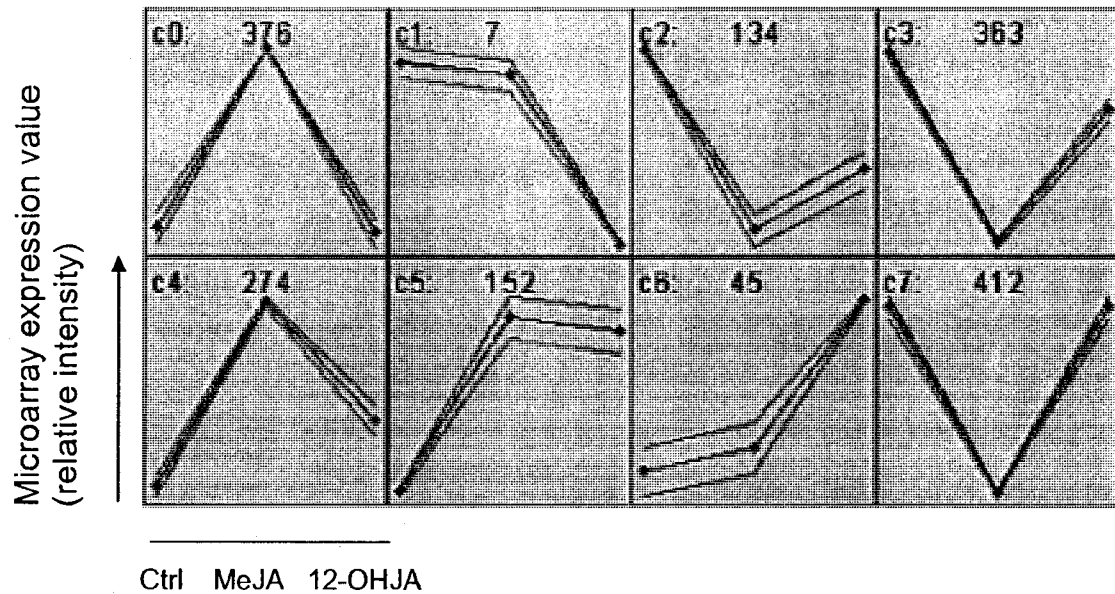


Figure 8: Cluster analysis of differentially expressed genes in *A. thaliana* control, 4h JAME or 4h 12-OH-JA treatments, represented by the three dots respectively. Clustering was performed using GeneCluster 2.1.7. The number above each graph indicates the number of genes in the respective cluster. The middle line shows the average gene expression pattern for the cluster, whereas the two outer lines represent the standard deviation in gene expression among the components of the clusters. Cluster 1 and 6 are especially interesting for the purpose of our analysis, as they indicate sets of genes regulated exclusively by 12-OHJA.

Table 3: Top 20 genes induced exclusively by MeJA

Accession	Identification	MeJA ^{17.6}		MeJA ^{18.6}		MeJA ^{18.1}		12-OHJA/	
		Control	MeJA	Control	MeJA	Control	MeJA	Control	OHJA/
At2g38240	putative anthocyanidin synthase	36.8	13813.6	100.6	375.7	2.7			
At1g76640	putative calmodulin similar to calmodulin	3.5	598.8	13.4	169.0	3.8			
At5g07010	steroid sulfotransferase-like protein AtST2a .	119.8	9743.6	222.9	81.3	1.9			
At4g22470	extensin - like protein hybrid proline-rich protein	12.2	809.6	50.1	66.2	4.1			
At1g10585	Expressed protein	58.8	3586.4	126.2	60.9	2.1			
At3g55970	leucoanthocyanidin dioxygenase -like protein	130.1	6956.3	90.1	53.4	0.7			
At2g34600	hypothetical protein predicted by genscan	13.5	695.2	94.8	51.4	7.0			
At1g35625	integral membrane protein, putative	6.5	291.3	57.8	44.5	8.8			
At1g15010	hypothetical protein	68.9	2794.2	72.5	40.6	1.1			
At1g63040	transcription factor DREB1A, putative	7.9	295.6	7.9	37.5	1.0			
At3g49620	putative protein SRG1 protein	147.0	4966.5	268.3	33.8	1.8			
At1g72260	thionin	104.4	3487.2	64.4	33.4	0.6			
At1g54020	myrosinase-associated protein, putative	71.5	2278.2	59.3	31.9	0.8			
At1g30135	Expressed protein	7.7	241.8	39.7	31.2	5.1			
At5g42900	putative protein similar to unknown protein	72.6	1905.1	68.8	26.2	0.9			
At2g27690	putative cytochrome P450	37.4	859.9	59.1	23.0	1.6			
At3g16330	unknown protein	16.1	362.6	16.0	22.6	1.0			
At5g42600	cycloartenol synthase	92.0	2036.9	241.8	22.1	2.6			
At3g50770	calmodulin-like protein flagellar	51.3	1089.8	62.9	21.2	1.2			

Table 4: Top 20 genes repressed exclusively by MeJA

Accession	Identification	Mean Control	Mean MeJA	Mean 12-OHJA	MeJA/control	12-OHJA/control
At3g27690	putative chlorophyll A-B binding protein	23907.72	235.74	24915.54	0.01	1.04
At5g45820	serine threonine protein kinase	3066.40	30.83	2578.21	0.01	0.84
At1g73870	hypothetical protein predicted by genscan+	573.99	6.68	445.12	0.01	0.78
At1g18970	germin, putative	720.40	14.83	582.71	0.02	0.81
At1g13650	unknown protein	1399.16	38.53	1289.24	0.03	0.92
At2g46830	MYB-related transcription factor (CCA1)	687.45	25.18	552.05	0.04	0.80
At1g30700	putative reticuline oxidase-like protein	449.65	17.97	361.58	0.04	0.80
At3g01550	putative phosphate/phosphoenolpyruvate translocator	713.54	37.21	580.37	0.05	0.81
At5g35970	DNA helicase-like	6573.73	345.61	5678.03	0.05	0.86
At1g32450	peptide transporter PTR2-B, putative	3167.07	208.79	2131.71	0.07	0.67
At4g11650	osmotin precursor	6190.56	413.49	4903.14	0.07	0.79
At3g12320	unknown protein	767.18	55.05	572.69	0.07	0.75
At3g54500	putative protein	1508.44	108.57	1427.05	0.07	0.95
At4g12980	putative protein hypothetical protein	2669.85	198.75	1666.54	0.07	0.62
	unknown protein contains similarity to alternative NADH-					
At1g07180	dehydrogenase	1219.88	91.48	1094.66	0.07	0.90
At2g46790	hypothetical protein predicted by genefinder	585.63	44.44	475.31	0.08	0.81
At3g13610	unknown protein contains similarity to DNA-binding protein	2089.90	160.08	2191.59	0.08	1.05
At4g19170	neoxanthin cleavage enzyme-like protein	7217.31	552.97	6744.08	0.08	0.93
At1g02205	hypothetical protein contains similarity to lipid transfer protein	4602.91	378.08	3700.77	0.08	0.80
At3g54040	photoassimilate-responsive protein PAR-1b -like protein	4428.07	371.02	3618.41	0.08	0.82

Table 5: Top 20 genes induced exclusively by 12-OHJA

Accession	Identification	Mean Control	Mean MeJA	Mean 12-OHJA	MeJA/control	12-OHJA/control
At4g15210	beta-amylase	107.90	161.28	1095.83	1.49	10.16
At2g47180	putative galactinol synthase	765.53	1590.64	7044.29	2.08	9.20
At4g18440	adenylosuccinate lyase - like protein	721.78	1939.53	6372.81	2.69	8.83
At1g56650	anthocyanin2, putative	124.15	104.32	931.73	0.84	7.50
At5g38120	4-coumarate--CoA ligase -like protein	88.02	206.54	503.74	2.35	5.72
At1g74930	AP2 domain containing protein, putative	144.62	218.52	647.24	1.51	4.48
At5g07700	transcription factor (gb AAD53097.1)	83.82	78.51	372.64	0.94	4.45
At3g12230	serine carboxypeptidase, putative	70.63	42.07	310.95	0.60	4.40
At4g19230	cytochrome P450 cytochrome P450	121.78	182.83	505.63	1.50	4.15
At1g20510	hypothetical protein	649.83	1195.42	2682.87	1.84	4.13
At1g75300	NADPH oxidoreductase	72.81	80.27	287.32	1.10	3.95
At5g48880	3-keto-acyl-CoA thiolase 2	2069.85	2209.97	8098.33	1.07	3.91
At5g22555	Expressed protein	207.24	21.88	717.27	0.11	3.46
At1g62540	similar to flavin-binding monooxygenase-like protein	239.54	323.90	796.96	1.35	3.33
At5g12340	putative protein	292.89	249.30	972.58	0.85	3.32
At3g06500	neutral invertase, putative	1090.46	1837.79	3379.73	1.69	3.10
At1g60270	beta-glucosidase, putative	113.20	312.08	339.52	2.76	3.00
At5g42800	dihydroflavonol 4-reductase	204.75	192.74	597.05	0.94	2.92
At4g37150	hydroxynitrile lyase like protein	226.18	192.15	650.60	0.85	2.88
At2g22200	AP2 domain transcription factor	148.00	244.68	424.92	1.65	2.87

Table 6: Seven genes repressed exclusively by 12-OHJA

Accession	Identification	Mean Control	Mean MeJA	Mean 12-OHJA	MeJA/control	12-OHJA/control
At1g18710	Myb-related transcription factor	390.78	331.45	29.26	0.85	0.07
At4g12490	pEARLI 1-like protein Arabidopsis thaliana	297.80	341.33	73.49	1.15	0.25
At4g12480	pEARLI 1	972.37	1443.28	291.07	1.48	0.30
At1g11545	endo-xyloglucan transferase, putative	697.33	464.13	265.65	0.67	0.38
At1g54740	hypothetical protein predicted by genscan+	494.30	381.44	216.36	0.77	0.44
At1g03870	unknown protein	3200.83	3180.42	1453.15	0.99	0.45
At2g47440	unknown protein	2070.65	2007.16	1170.05	0.97	0.57

Table 7: Top 20 genes induced by both MeJA and 12-OHJA

Accession	Identification	Mean Control	Mean MeJA	Mean 12-OHJA	MeJA/control	12-OHJA/control
At4g17470	putative protein	688.73	8958.15	13057.11	13.01	18.96
At5g36220	cytochrome P450	223.70	2582.09	2046.97	11.54	9.15
At4g13410	putative protein Cyclic beta-1-3-glucan synthase	96.78	1039.11	573.13	10.74	5.92
At1g52890	NAM-like protein similar to NAM (no apical meristem)	131.72	1362.10	665.70	10.34	5.05
At4g23600	tyrosine transaminase like protein	3172.50	30676.11	21611.41	9.67	6.81
At1g19180	unknown protein	980.55	9405.17	6182.59	9.59	6.31
At4g21830	putative protein	814.68	7296.73	8278.61	8.96	10.16
At5g06870	polygalacturonase inhibiting protein	1398.87	11402.43	9435.80	8.15	6.75
At3g28740	cytochrome P450, putative contains Pfam profile	857.72	6874.54	4768.27	8.01	5.56
At3g44860	AIPP -like protein	557.78	4253.60	4000.90	7.63	7.17
At1g53885	Expressed protein	520.98	3869.57	4718.74	7.43	9.06
At2g38750	putative annexin	421.91	3096.80	3115.04	7.34	7.38
At1g70700	hypothetical protein predicted by genefinder	1137.04	8168.79	7561.19	7.18	6.65
At1g32640	protein kinase, putative identical to bHLH protein	867.55	5910.25	4742.25	6.81	5.47
At5g66650	putative protein contains similarity to unknown protein	95.69	632.63	284.95	6.61	2.98
At1g74950	unknown protein	1070.08	6615.75	4722.25	6.18	4.41
At3g51450	mucin -like protein hemomucin	609.31	3692.50	2807.54	6.06	4.61
At2g43530	putative trypsin inhibitor	2065.93	12357.65	5702.60	5.98	2.76
At1g44350	IAA-amino acid hydrolase, putative	691.89	4106.35	3458.76	5.93	5.00
At2g06255	Expressed protein	37.96	219.90	209.41	5.79	5.52

Table 8: Top 20 genes repressed by both MeJA and 12-OHJA

Accession	Identification	Mean Control	Mean MeJA	Mean 12-OHJA	MeJA/control	12-OHJA/control
At1g49860	glutathione S-transferase, putative	830.24	12.71	140.94	0.02	0.17
At3g18200	integral membrane protein, putative similar to MtN21	291.74	13.76	131.75	0.05	0.45
At2g41800	unknown protein	280.16	16.97	107.04	0.06	0.38
At5g12940	putative protein DRT100 protein precursor	355.17	23.12	198.47	0.07	0.56
At3g24290	ammonium transporter, putative	519.11	37.33	216.63	0.07	0.42
At5g10130	pollen allergen -like protein SAH7 protein	193.88	15.50	50.97	0.08	0.26
At5g62340	putative protein 21K protein precursor, Medicago sativa	518.21	42.20	117.21	0.08	0.23
At1g51860	receptor-like protein kinase, putative	222.93	19.04	72.90	0.09	0.33
At5g67430	N-acetyltransferase hookless1-like protein	239.71	21.23	172.84	0.09	0.72
At5g02780	putative protein In2, Zea mays,	286.72	25.88	117.20	0.09	0.41
At5g56080	nicotianamine synthase	556.82	50.82	150.24	0.09	0.27
At5g62210	embryo-specific protein - like embryo-specific protein 3	456.59	42.72	152.85	0.09	0.33
At4g26320	putative protein	409.97	40.42	176.82	0.10	0.43
At4g36610	putative protein	261.62	26.59	133.56	0.10	0.51
At2g21650	unknown protein	328.50	35.69	224.84	0.11	0.68
At2g44380	unknown protein	758.92	82.78	231.96	0.11	0.31
At3g51330	putative protein	502.44	55.34	209.90	0.11	0.42
At4g17280	hypothetical protein	419.08	46.20	196.80	0.11	0.47
At5g63660	putative protein	278.50	31.07	117.01	0.11	0.42
At2g19970	putative pathogenesis-related protein	804.97	92.40	317.81	0.11	0.39

Table 9: Comparison of experimental values to known MeJA-induced genes

Accession #	Gene Name	Genevestigator microarray data collection*		Current Experiment	
		Ratio MeJA	Ratio MeJA	Ratio MeJA	Ratio 12-OHJA
At5g24780	VSP1	13.37	2.37	2.89	
At5g44420	<i>Pdf1.2</i> **	0.95	6.56	0.39	
At1g72260	<i>Thi2.1</i>	3.36	33.40	0.62	
At5g44420	<i>thionin, putative</i> ***	14.09	1.23	2.43	
At1g19670	<i>chlorophyllase 1 (CLH1)</i>	30.83	4.71	2.83	
At5g67300	<i>myb-related protein</i>	2.67	2.61	1.95	
At1g06180	<i>MYB-related protein</i>	1.62	3.20	1.47	
At3g45140	LOX2		3.7	3.2	
At2g06050	OPR3	9.45	4.96	5.22	
At5g42650	AOS	9.83	4.72	3.44	
At1g13280	AOC	2.41	1.90	1.85	
At5g66170	<i>senescence-associated protein</i>	1.61	2.89	1.30	
At4g35770	<i>senescence-associated protein sen1</i> **	0.94	4.13	1.18	
At2g34930	<i>putative disease resistance protein</i>	3.62	3.92	4.20	
At1g72940	<i>disease resistance protein, putative</i>	3.31	2.62	0.99	

* Genevestigator disclaimer: Since in some cases, two or more experiments studying the same effect were pooled to cover more tissue types (in fact, the responses of some genes may not appear in one experiment, but do in another experiment performed on other tissue types).

**These genes are known to be induced by MeJA. The Genevestigator data may be different for two reasons: the conditions of the experiment are slightly different than our own (i.e. the treatment was performed for 1 and 3h with 10 μ M MeJA) and the resulting data is that of a pool of the two treatments, or that there can be errors even in available data for comparison.

**This putative thionin gene is seen in our experiment to be induced only by 12-OHJA. As *Thi2.1* is not induced in the 12-OHJA presence, this alternate thionin can show internal specificities for the differential bioprocessing of MeJA and 12-OHJA.

Table 10: Comparison of experimental values to known MeJA- repressed groups of genes

Accession #	Gene Name	Genevestigator microarray data collection*		Current Experiment	
		Ratio MeJA	Ratio	Ratio MeJA	Ratio 12-OHJA
At3g47470	Chlorophyll AB binding protein	0.80		0.35	1.10
At3g27690	putative chlorophyll A-B binding protein	0.90		0.01	1.04
At3g08940	putative chlorophyll a/b-binding protein	0.08		0.19	1.02
At2g05070	putative chlorophyll a/b binding protein	0.82		0.09	1.06
At5g54270	Lhcb3 chlorophyll a/b binding protein	0.74		0.21	1.05
At1g44446	chlorophyll a oxygenase	0.82		0.13	0.92
At5g54190	NADPH:protochlorophyllide oxidoreductase A	0.99		0.10	1.10
At3g52720	carbonic anhydrase (CAH1)	0.41		0.32	0.49
At5g17330	glutamate decarboxylase 1 (GAD 1)	0.95		0.31	0.85
At5g14260	putative protein ribulose-1,5-bisphosphate carboxylase/oxygenase N-methyltransferase	0.89		0.45	0.96
At3g14930	uroporphyrinogen decarboxylase, putative	0.92		0.34	0.96
At2g46830	MYB-related transcription factor (CCA1)	0.95		0.04	0.80
At5g08330	putative protein auxin-induced transcription factor	0.69		0.31	0.86
At5g07690	transcription factor-like protein	1.36		0.43	1.34
At4g29190	putative protein Zn- finger transcription factor	0.54		0.40	1.11
At1g71030	putative transcription factor similar to myb-related transcription factor 24	0.49		0.19	1.09

3.1.3 RT-PCR Validation of Microarray Data

To ensure that the microarray results are reliable, we needed to verify them by the use of another method to prove that the genes are indeed behaving according to the reported patterns. Our method of choice was RT-PCR, an easy and cheap method, once a good internal control is achieved. Since optimization using one internal control gene (Actin 4) proved troublesome, new primers were designed to amplify 8 of the actin genes at the same time, in order to reduce variance (individual actin gene expression may fluctuate between the treatments used in this study). We selected genes representative of different clusters, mRNA levels were detected and the results compared to the Affymetrix data. RT-PCR results and associated microarray values can be seen in Figure 9 and Table 11, respectively.

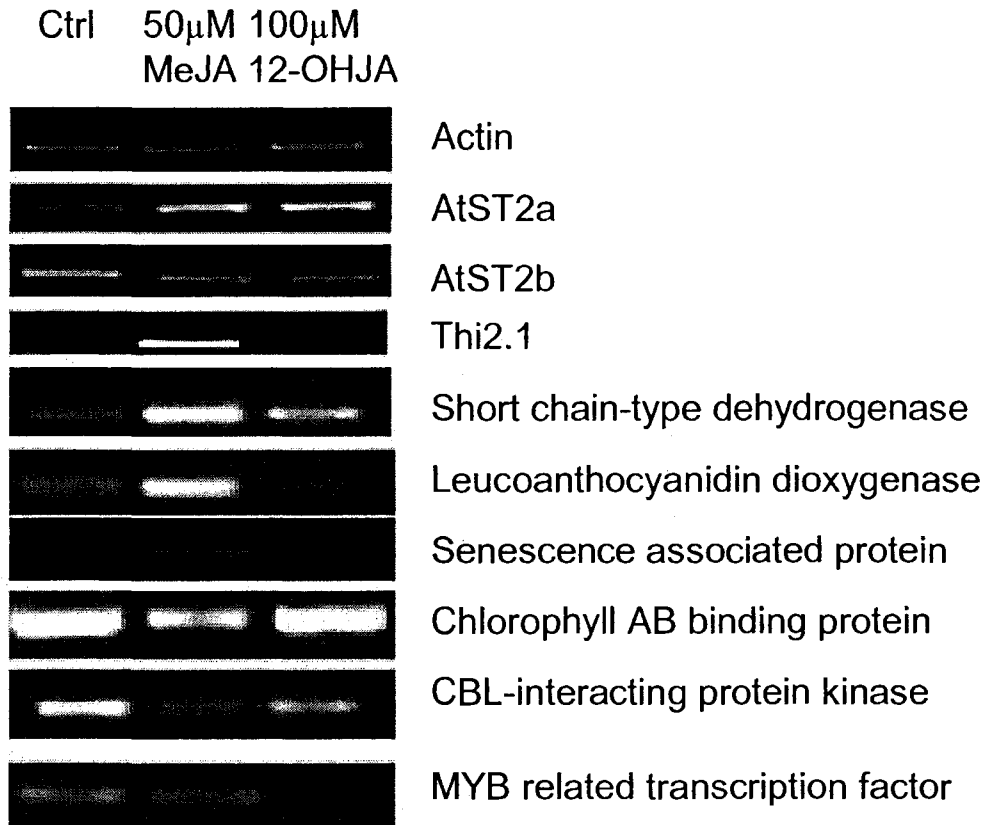


Figure 9: RT-PCR validation of microarray experiment in Col0 ecotype for control and plants treated with 50µM MeJA or 100µM 12-OHJA for 4 hours.

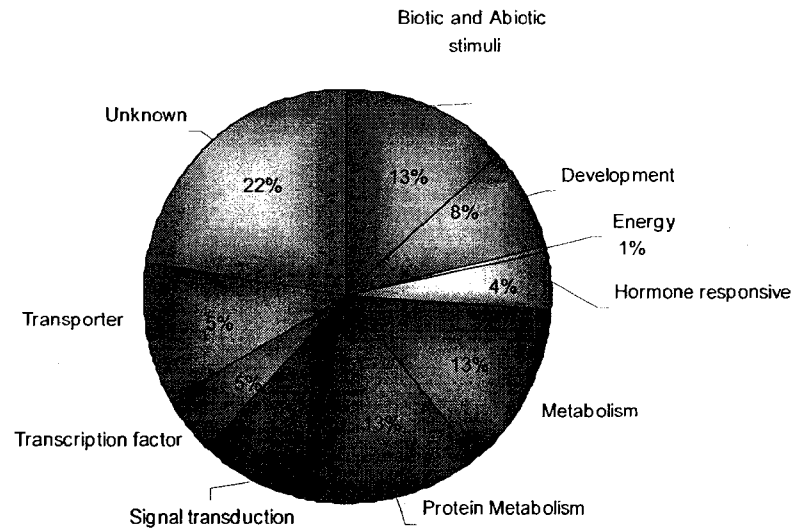
Table 11: Affymetrix array expression values

Gene	Gene # ID	Mean Control	Mean MeJA	Mean 12-OHJA
AtST2a	At5g07010	119.8	9743.6	222.9
AtST2b	At5g07000	236.4	389.7	182.7
Thi2.1	At1g72260	104.4	3487.2	64.4
Short chain-type dehydrogenase	At3g04000	175.5	3747.6	364.9
Leucoanthocyanidin dioxygenase	At3g55970	130.1	6956.3	90.1
Senescence associated protein	At2g17850	68.2	93.4	4.6
Chlorophyll AB binding protein	At3g27690	23907.7	235.7	24915.5
CBL-interacting protein kinase	At5g45820	3066.4	30.8	2578.2
MYB related transcription factor	At1g18710	390.8	331.4	29.3

3.1.4 Biological functions of various clusters

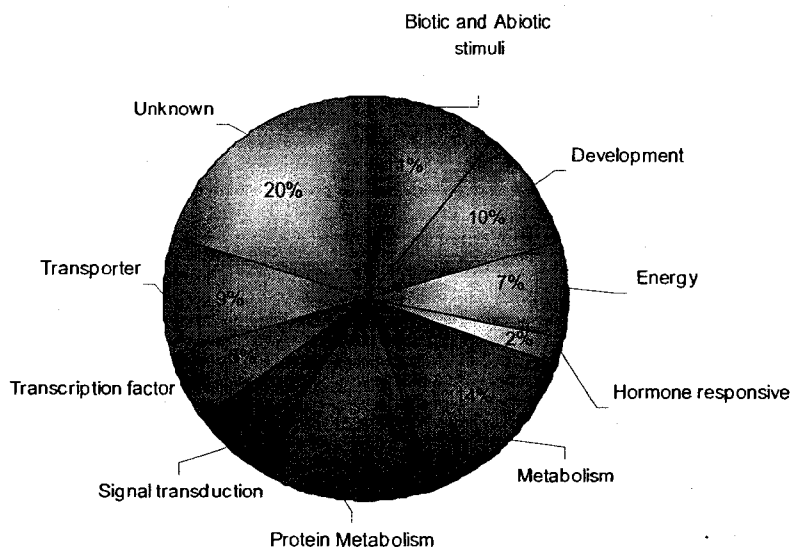
To gain further insight into the function of the genes regulated by each of the compounds, the 1763 significant genes were manually categorized into a maximum of 10 functional groups using the gene ontology (GO) annotation data from the Affymetrix web site at <http://www.A.thalianai.org/tools/bulk/go/index.jsp>, combined with some manual modifications. The exact distribution of genes in these biological processes can be seen in Figures 10, 11 and 12.

A. Cluster 0 (↑ MeJA)



Total # of genes : 376
 Total # of matching probes : 365

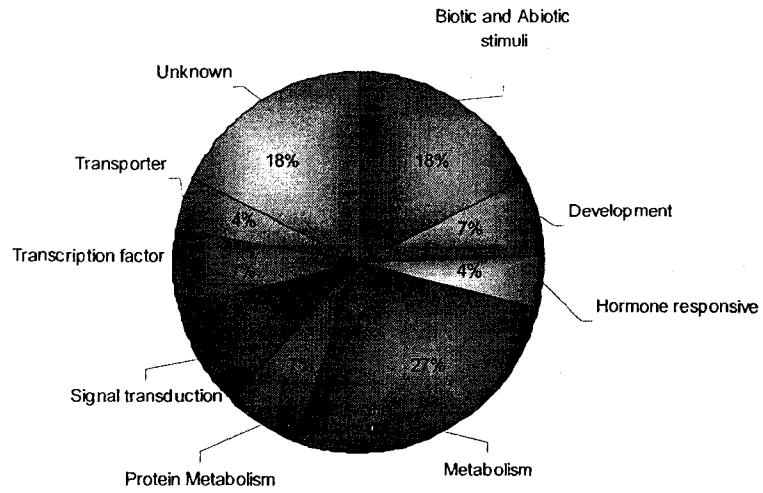
B. Cluster 7 (↓ MeJA)



Total # of genes : 412
 Total # of matching probes : 411

Figure 10: Classification of A) 365 MeJA up-regulated and B) 411 MeJA down-regulated genes into functional groups based on their known, predicted and/or putative biological function.

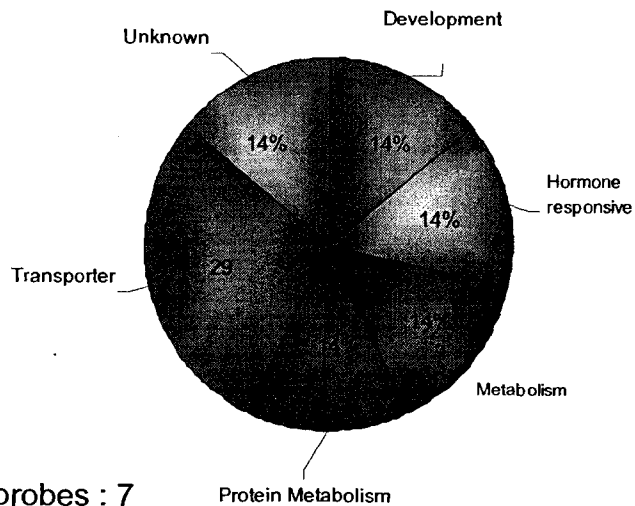
A. Cluster 6 (↑ 12-OHJA)



Total # of genes : 45
 Total # of matching probes : 45

Cluster 1 (↓ 12-OHJA)

B.

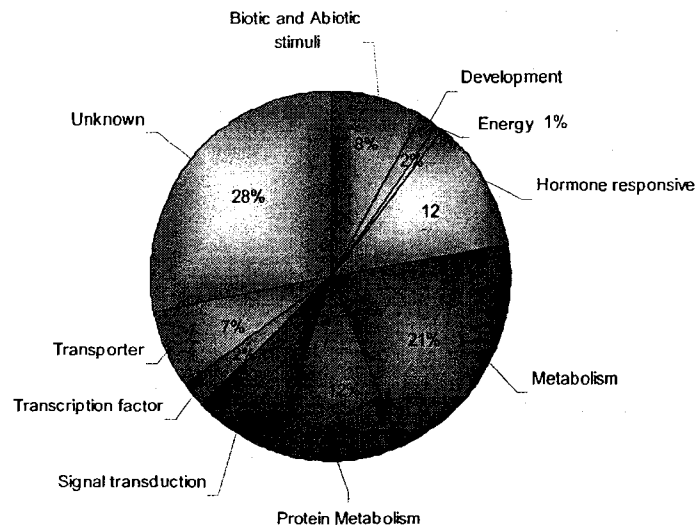


Total # of genes : 7
 Total # of matching probes : 7

Figure 11: Classification of A) 45 12-OHJA up-regulated and B) 7 12-OHJA down-regulated genes into functional groups based on their known, predicted and/or putative biological function.

A.

Cluster 5 (↑↑ MeJA and 12-OHJA)

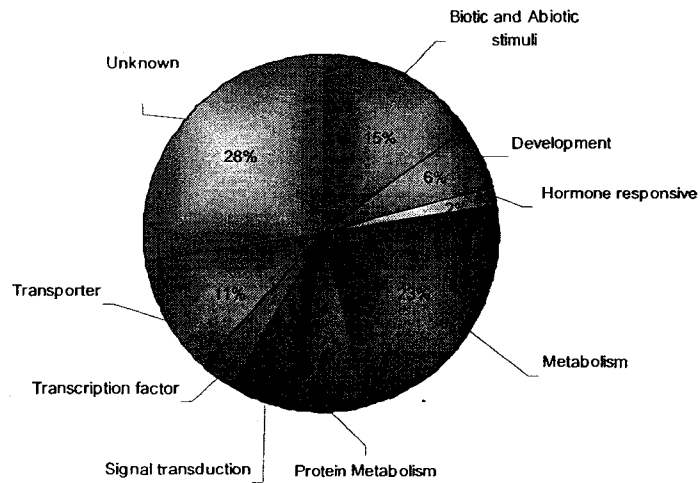


Total # of genes : 152

Total # of matching probes : 145

B.

Cluster 2 (↓↓ MeJA and 12-OHJA)



Total # of genes : 134

Total # of matching probes : 120

Figure 12: Classification of A) 145 up-regulated and B) 120 down-regulated genes in response to both MeJA and 12-OHJA treatments into functional groups based on their known, predicted and/or putative biological function.

3.2 Positioning of the *AtST2a* and *AtST2b* genes in the floral pathway

In addition to being induced by the two aforementioned compounds, MeJA and 12-OHJA, *AtST2a* is known to be regulated by photoperiod, by also being induced following 8 h of dark treatment (Levitin, 2004). Nothing was known prior to this study regarding regulation of *AtST2b*. In order to determine more precisely where these two genes are situated in the flower regulation pathway (see Figure 2), the gene expression profile of *AtST2a* and *AtST2b* was determined under wildtype and 48h dark treatment conditions in various flowering time mutant plants. The mutants were selected either for their mutation in the internal clock response to light (*CO-2*, *Toc1*), or in the temperature signal integration on growth (*Fca1*, *Fca1*- different alleles of the same mutation). The wild-type background for each mutant was included as control, and the results are seen in Figure 13.

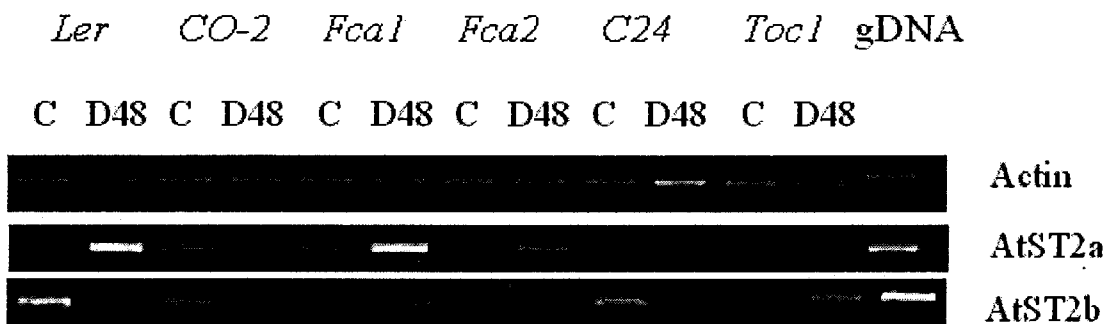


Figure 13: Patterns of *AtST2a* and *AtST2b* gene expression in different flowering time mutants and their wildtype background. Plants exposed to wildtype (control- C) conditions or dark-treated for 48 h (D48) were studied for the expression patterns of *AtST2a* and *AtST2b* mRNA.

The results show that *AtST2a* is no longer induced in the dark in the light perception mutants *CO-2* and *Toc1*, but is still responsive to the treatment in the autonomous pathway mutants, *Fca1* and *Fca2*.

3.3 Molecular and Phenotypic Characterization of *AtST2a* and *AtST2b* Knockout Lines

3.3.1 Introduction

Histochemical analysis of plants transformed with the GUS reporter fused to the *AtST2a* promoter revealed the regions of expression of the *AtST2a* gene (Levitin, A, 2004). The plants showed the highest GUS levels in mature seeds, but not immature seeds, emerging leaves, tips of growing leaves, base of trichomes, root apical meristem and emerging lateral roots, plant apical meristem and floral primordia (Levitin, A, 2004), all sites of cell division and/ or differentiation. This points towards a possible role for its substrate, 12-OHJA, in these processes and the compound's regulation through sulfonation by *AtST2a*.

Additionally, transgenic lines carrying the *AtST2a* gene in the sense and antisense orientation showed differential flowering time compared to wildtype plants (Gidda, S, 2003). Under short days, plants overexpressing the enzyme flowered later, whereas plants expressing the gene in the antisense orientation flowered early. There seems to be therefore a link between 12-OHJA and/or 12-OHJA-SO₄ levels and flower initiation.

The accumulating evidence toward a role for 12-OHJA in plant development made us seek knockout lines to investigate the phenotype of increased and decreased 12-OHJA sulfate levels in an *AtST2a*- KO plant. Furthermore, we wanted to compare the *AtST2a*- KO phenotype with the one of a loss of function in a highly similar sulfotransferase, *AtST2b*, whose substrate is

yet to be identified. Previous data allowed us to better direct our phenotypic studies towards the sites of expression determined by the GUS-*AtST2a* promoter analysis, and investigate the phenotype that seemed to characterize the transgenic lines, i.e. flowering time.

3.3.2 Molecular Characterization of *AtST2a*- and *AtST2b*- KO lines

The T-DNA mutants at the Salk Institute come with an alignment and annotation of the insertion site and the best approximation of where the T-DNA insert is located (5'UTR, exon, intron, 3'UTR). Gene annotation is then made accessible via a web-interface to researchers with ease of access to mutants in their gene of interest. Exact positioning of the insertion site is possible through sequence alignments of the sequencing product with the *A. thaliana* genome. Investigators are cautioned to confirm the presence of the expected T-DNA insertion using PCR, and any additional method available to test the disruption of the gene is encouraged.

Seeds obtained from the GAB-KAT collection for the *AtST2a*-KO and the Salk Institute for the *AtST2b*-KO were grown in soil until enough material was available for gDNA extraction. PCR experiments on samples from 20 plants of each mutant were conducted in order to find a homozygous mutant for each gene. Several homozygous mutants were identified, and two were selected for further studies.

AtST2a- KO plant 15 and *AtST2b*- KO plant 45, as well as their progeny, were confirmed homozygous KOs by triplicate PCRs. Figure 14 shows a fragment when the gDNA was amplified with the appropriate gene-specific and T-DNA specific primers, but no band was observed with the gene specific primers only. Actin4 primers were used as positive control for amplification, while the *Col0* ecotype was the control for the gene and T-DNA specificity.



Figure 14: PCR determination of homozygous *AtST2a* and *AtST2b* mutant lines. The results show that although the *AtST2a* primers were functional (*Col0*-2A lane), no amplification is seen in the *AtST2a*- KO plant 15 (hereon referred to as *AtST2a*- KO). The same is true for the *AtST2b* gene in the *AtST2b*-KO Line 45 (hereon *AtST2b*- KO). When appropriate gene-specific and the T-DNA left border primer were used, a band is seen in both mutants confirming the presence of an insert in the gene, both by the presence and the size of the PCR product.

3.3.3 Genetic analysis of *AtST2a*-KO and *AtST2b*-KO

In order to gain more insight into the functions of our two sulfotransferases, we looked at the regulation of genes in the JA pathway in the two mutants, as compared to their wildtype background, *Col0* (Figure 15). The *coi1-16* mutant was included as a comparison for what is expected in a JA deficient mutant, versus a mutant which accumulates one of the downstream members of the JA-family, 12-OHJA. The *PorA* gene was included in the RT-

PCR for its known repression in the dark, in light of our own genes' regulation by photoperiod, as control for the dark treatment.

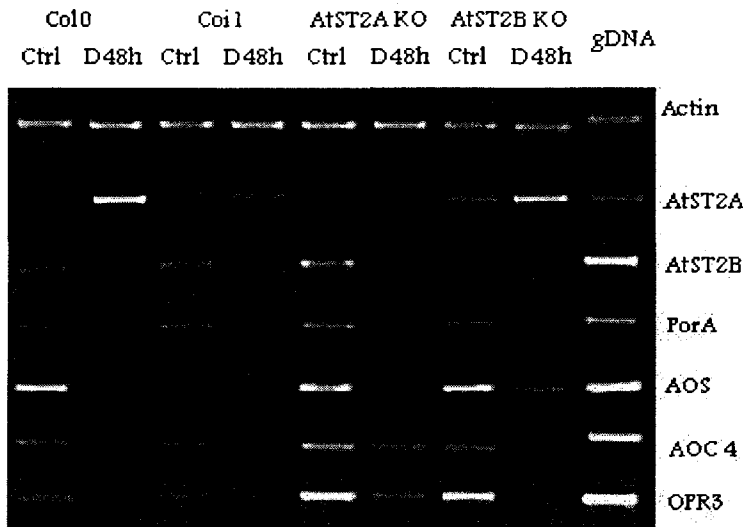


Figure 15: RT-PCR results of gene expression patterns of photoperiod (*PorA*) and jasmonate pathway (*AOS*, *AOC4* and *OPR3*) genes in wildtype, *coi1-16*, *AtST2a-KO* and *AtST2b-KO*.

3.3.4 Metabolite Characterization of *AtST2a* and *AtSt2b* KO lines

Investigating the metabolite content of the KO lines in terms of 12-OHJA-SO₄ has a dual role: first to verify by yet another means that the function of *AtST2a* is indeed to sulfonate the 12-OHJA molecule, and second, to confirm that the function is disrupted in our mutant line. *AtST2b* –KO was also included in the analysis to detect any possible differences in terms of the two metabolites mentioned above, although the data so far indicates no function for this enzyme in 12-OHJA metabolism.

In order to do this, wildtype and knockout plants were grown for 16 days, treated for 48 h with 100 μ M MeJA for *AtST2a* induction in the control, and total metabolites were extracted. Following HPLC purification, samples were injected on a Quattro triple quadrupole mass spectrometer (Micromass, UK) using neutral loss ESI-mass spectrometry in the negative mode, in search of a parent ion with a molecular mass at 305 (M-1), losing a neutral fragment of 80 Daltons, corresponding to the sulfonyl group.

3.3.4.1 HPLC Purification

The first thing to determine was the elution time of 12-OHJA-SO₄ in the HPLC gradient (see Materials and Methods). A sample of the reaction product catalyzed by *AtST2a* with 12-OHJA in the presence of [³⁵S]-labelled PAPS was thus analyzed and the results can be seen in Figure 16.

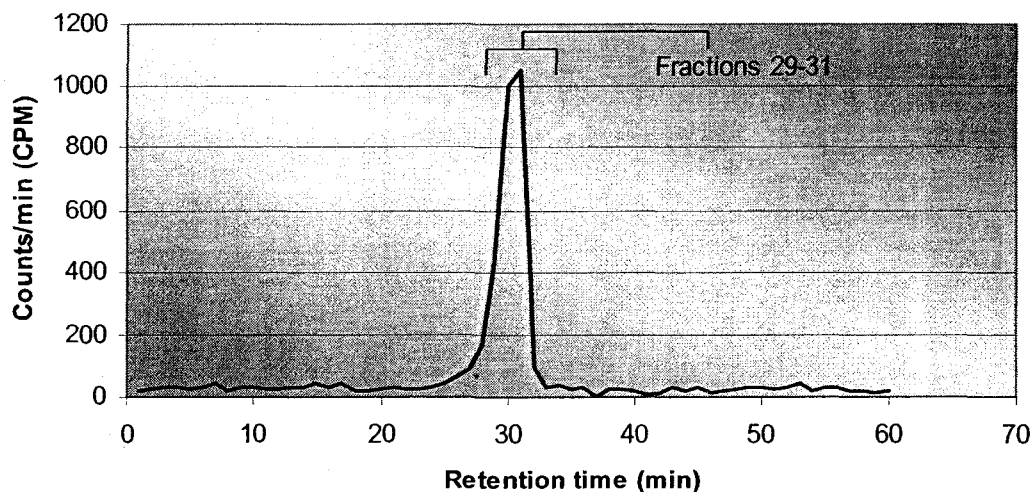


Figure 16: HPLC elution profile of 12-OHJA-³⁵SO₄. Fractions 29, 30 and 31 were shown to contain the radioactive product.

3.3.4.2 Mass Spectrometry of Purified Fractions

Having determined that 12-OHJA-SO₄ elutes in fractions 29-31 allowed us to isolate these fractions from the pool of metabolites present in the three extracts (Col0, *AtST2a*- KO and *AtST2b*- KO) and subject them to mass spectrometry. The results of neutral loss MS spectras in negative mode can be seen in Figure 17.

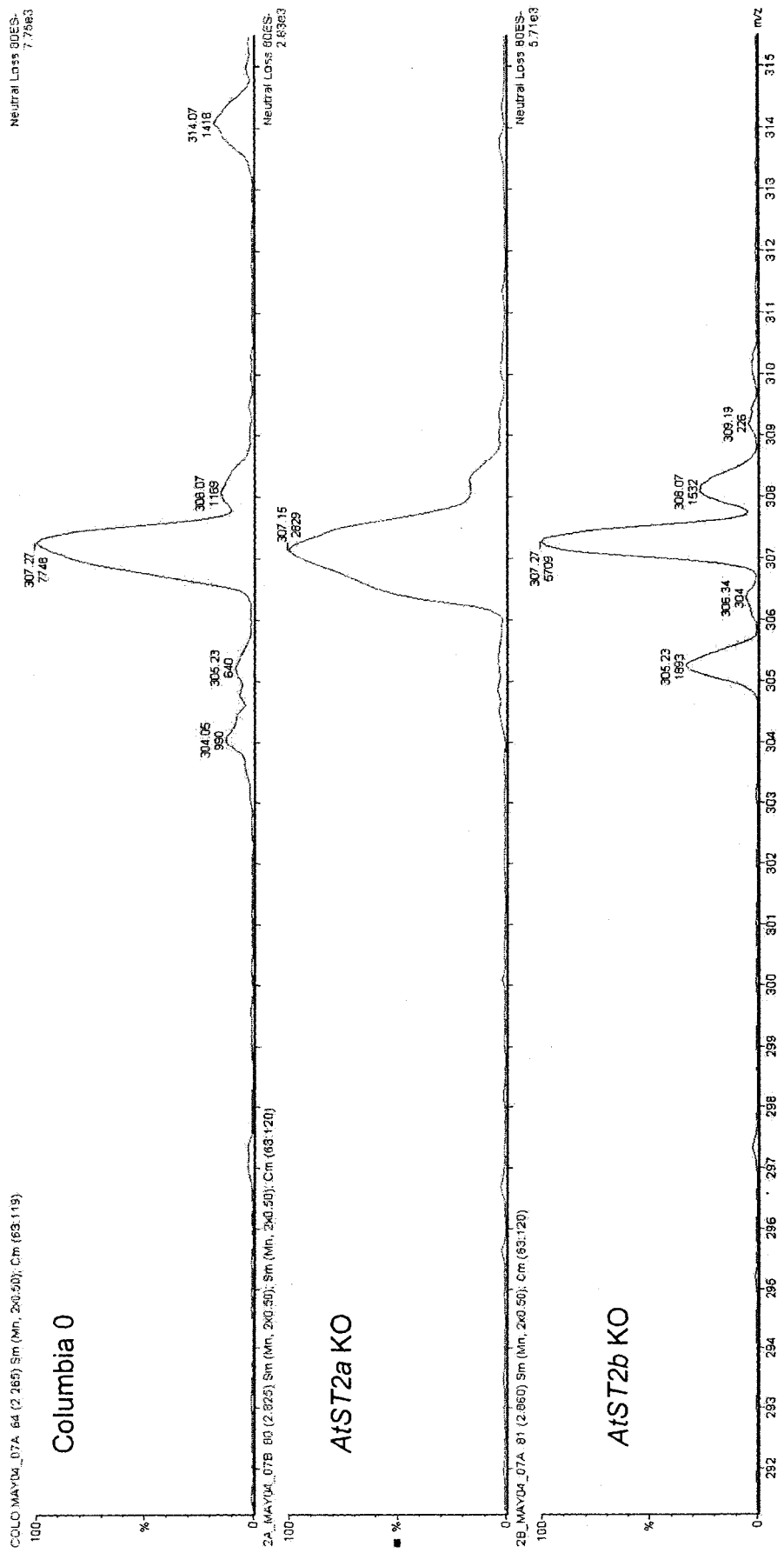


Figure 17: Neutral loss spectrum of wildtype and KO mutants showing presence or lack of 12-OHJA-SO₄ (mw 305). The peak representing 12-OHJA-SO₄ at 305Da is present in the wildtype plants (Columbia 0), but disappears in the AtSt2a- KO, confirming that the sulfotransferase function is indeed disrupted in this mutant. In the AtST2b- KO plants, the metabolite seems to be more abundant than in wildtype plants, if we consider relative amounts between the 305 and 307 ions.

As expected, the peak at 305 (M-1), corresponding to the sulfonation product of 12-OHJA by the AtST2a enzyme is missing in the *AtST2a*- KO background, but is present both in wildtype and *AtST2b*- KO. Additionally, a peak at 307 has been observed in all three extracts. To investigate if the new peak belongs to the jasmonates family, or is something else that just elutes at the same time in the HPLC gradient, the MS-MS fragmentation pattern for both peaks was determined on a MS spectrometer (Figure 18).

The fragmentation pattern of the 305 ion was found to correspond exactly to the fragments obtained with authentic 12-OHJA sulfate. Interestingly, the fragmentation pattern of the 307 ion gave some fragments identical to the ones of the 305 ion. The other fragments have an additional 2 Daltons in their mass, corresponding to the presence of 2 hydrogen atoms. This new metabolite is thus proposed to be the reduced form of 12-OHJASO₄ (see Figure 19).

Metabolite analysis of transgenic lines previously available in the lab overexpressing the two genes in the sense or antisense orientation was also performed (Figure 20). The results confirmed that the *AtST2a* overexpressing line (S9) was true, but expressing the gene in the antisense orientation (733) was not enough to remove any traces of 12-OHJA sulfate. Overexpression of *AtST2b* in the sense (S6-6) or antisense (16-6) modified the relative pools of 305 and 307 ions present, but more analysis is required to understand the significance of this.

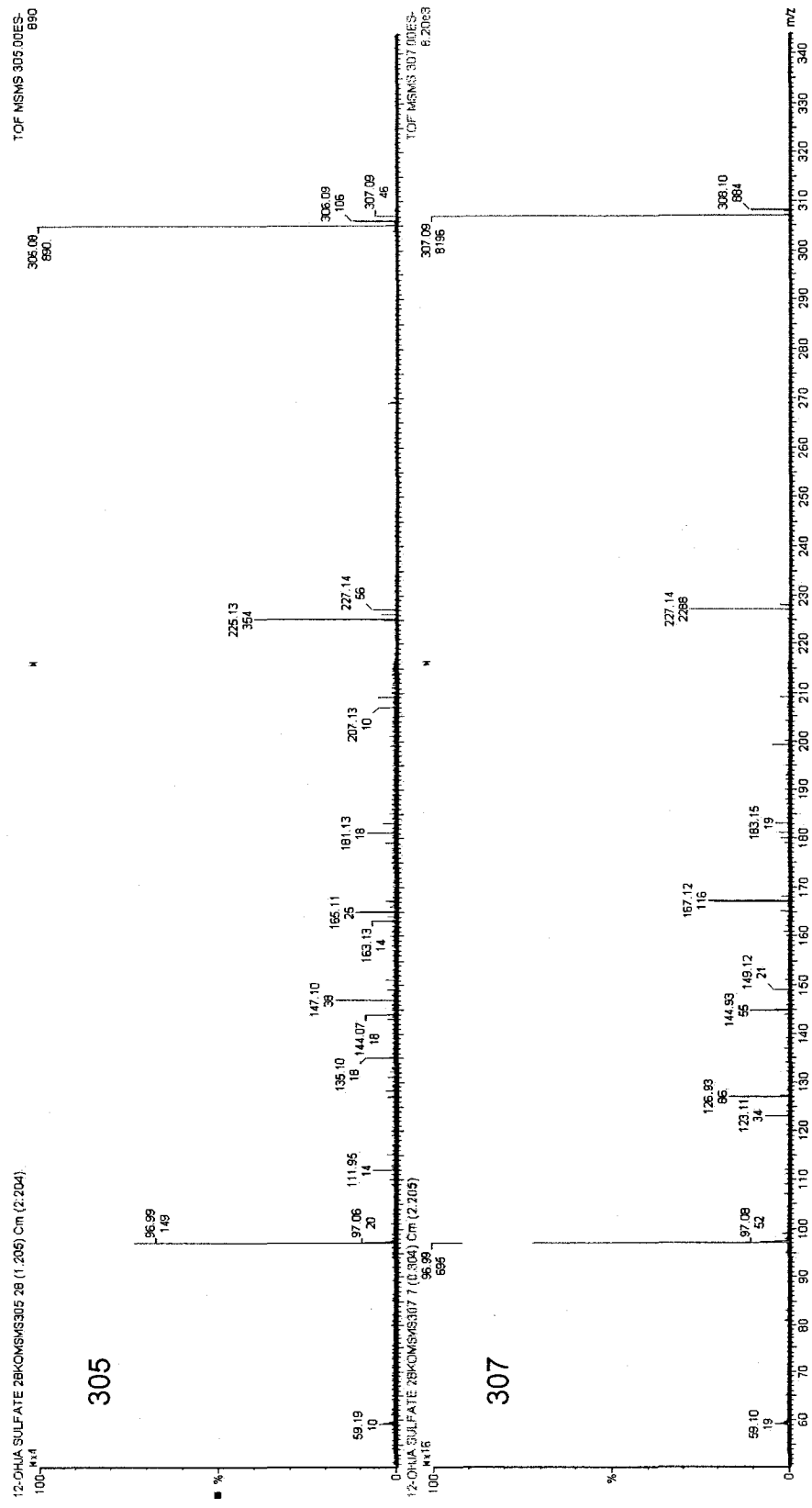


Figure 18: Fragmentation patterns of the 305 and 307 ions by MS/MS spectrometry. Some fragments of both molecules have the same mass as the 12-OHJA molecule (see peaks 59 and 97), while others have an additional charge of two Daltons (147 corresponds to 149, 165 to 167, 225 to 227, etc).

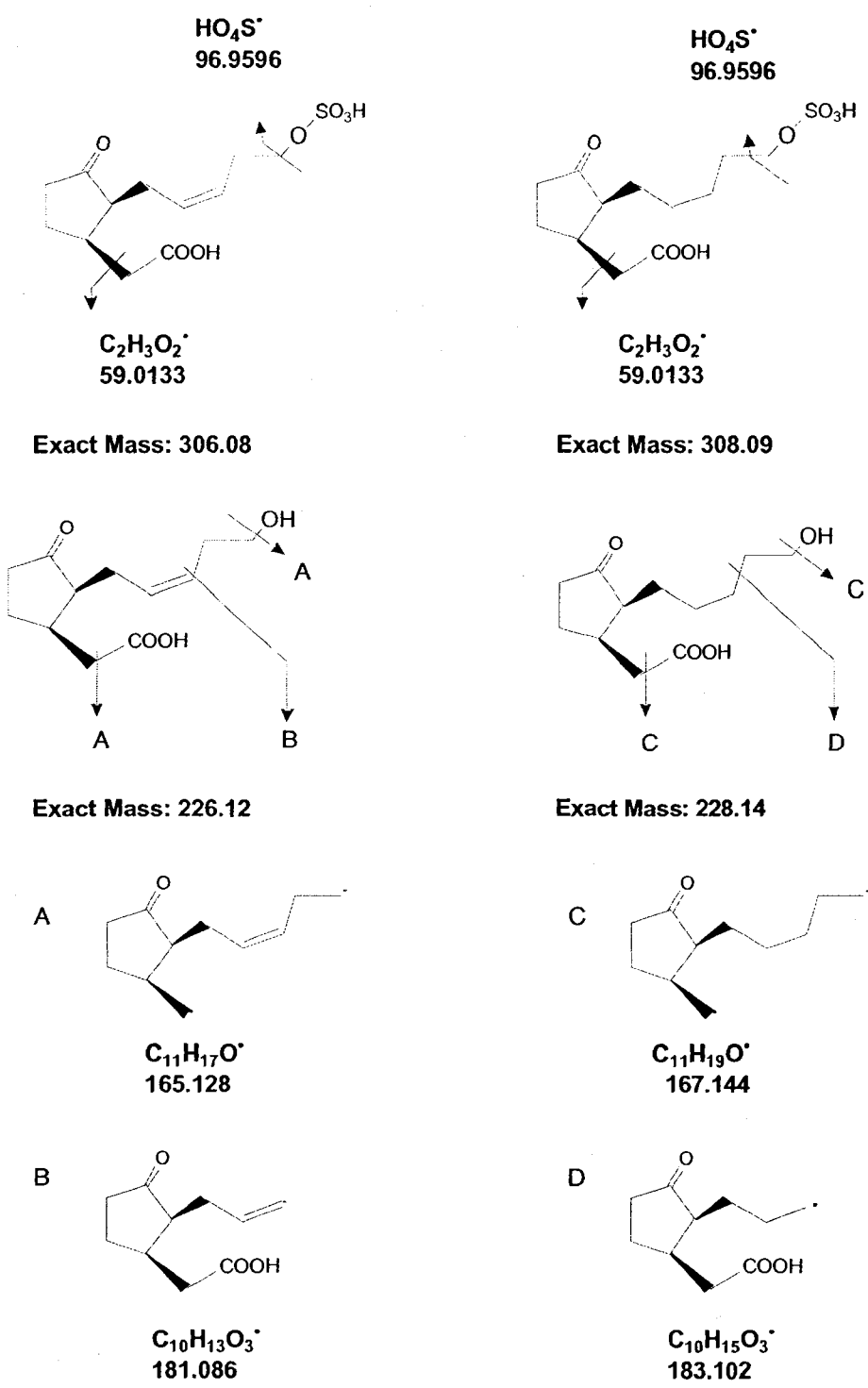


Figure 19: Exact mass of 12-OHJA-SO₄ and broken down fragments in negative mode. Left: double bond in the side chain Right: reduced double bond in the side chain

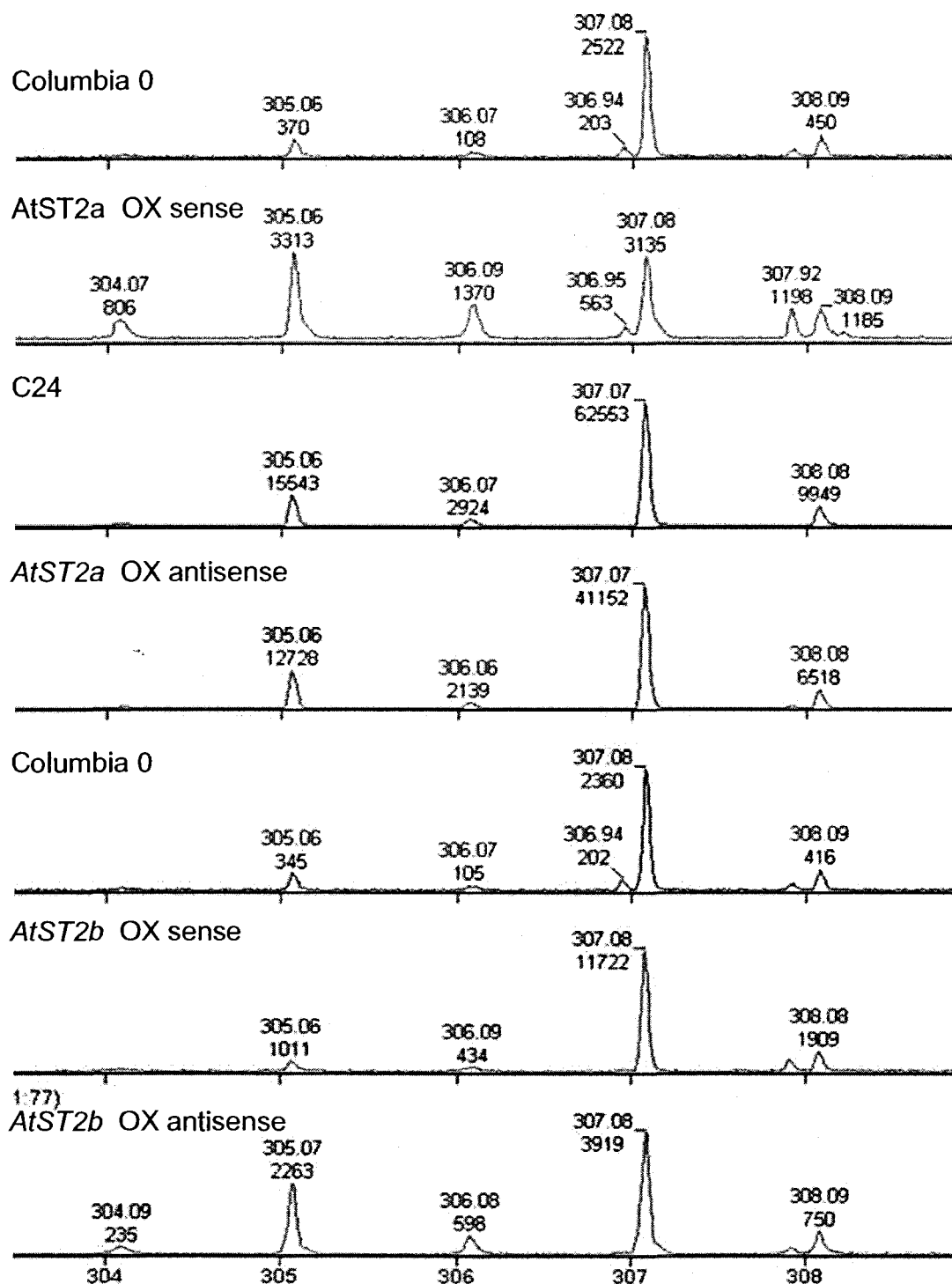


Figure 20: Mass spectra of AtSt2a and AtST2b overexpressing and antisense lines and their respective wildtype control, in negative mode. Comparing the metabolite content of the AtSt2 transgenic lines to their wildtype background in terms relative abundance of the two related compounds allowed us to determine that some lines are real transgenic (eg. *AtST2a* OX sense), while others aren't (eg. *AtST2a* OX antisense). The results for the *AtST2b* OX lines suggest an implication of *AtST2b* in the sulfonation of the new metabolite, with overlap of function with *AtST2a*.

3.4 Phenotypic Analysis of *AtST2a* and *AtSt2b* KO lines

3.4.1 Effect on Germination Time

Following the isolation of homozygous KO lines for both genes, we looked first at their germination time and percentile, based on the fact that *AtST2a* mRNA accumulated in mature seeds, and previous *AtST2a* antisense line showed a drastically reduced germination rate. For both KO lines, average seed germination time (Table 12) and percentile (Table 13) were identical to the wildtype.

Table 12: Knockout plants grown in soil, independently of photoperiod, germinate at the same time as the wildtype control.

Ecotype (N=32)	Germination day and probability (p) value as compared to wildtype	
	Long Day	Short Day
Col0	2.866	3.125
<i>AtST2a-KO</i>	3.063 (p=0.0969)	3.312 (p=0.1957)
<i>AtST2b-KO</i>	2.725 (p=0.1238)	3.063 (p=0.1214)

Once the average germination time had been determined, we decided to investigate the percent seed germination on that day on regular growth medium (MS) or media supplemented with various concentrations of MeJA. The results can be seen in Table 13, and Figure 21. Due to the known insensitivity of the *coi1-16* mutant to the presence of MeJA, this ecotype was included in the experiment as a negative control for the effect of MeJA on germination. Both *AtST2a* and *AtST2b* KO lines showed increased sensitivity to increasing

concentrations of MeJA (figure 22), suggesting that they might play a role in the detoxification of excess jasmonates.

Table 13: Percent germination assessed on day 3 on MS medium, or MS media supplied with 25, 50 or 100µM MeJA (n=12).

Ecotype	MS (control)	MS+ 25µM MeJa	MS+ 50µM MeJa	MS+ 100µM MeJa
<i>Columbia 0</i>	100	92	100	100
<i>AtST2a-KO</i>	90	89	73	70
<i>AtST2b-KO</i>	92	92	67	25
<i>coi1-16</i>	100	100	100	100

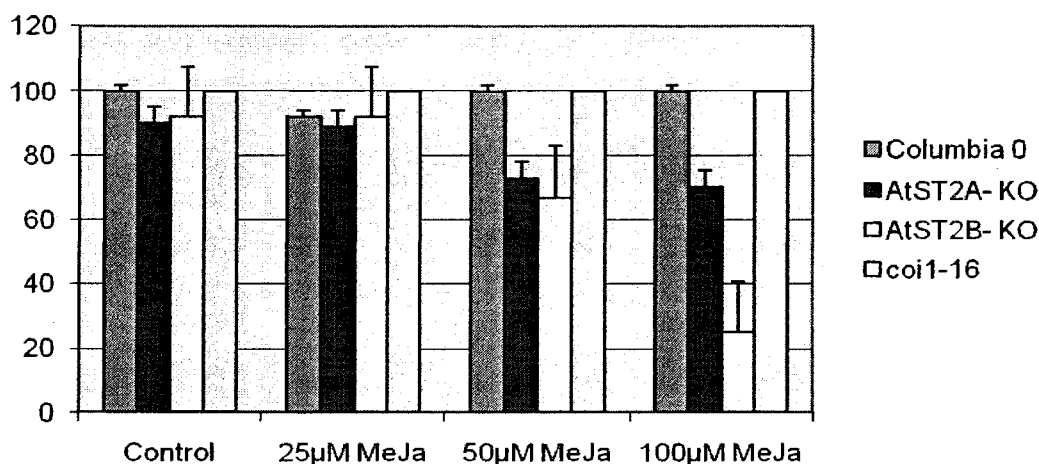


Figure 21: Graphical representation of the germination percentile of the wildtype ecotype *Columbia 0*, as well as the *AtST2a*- and *AtST2b*- KOs and the JA-insensitive *coi1-16* mutant on MS media and MS medium containing various concentrations of MeJA.

3.4.2 Effect on Root Emergence

We further observed that seeds that had germinated in the two knockout mutants on MS media supplemented with 100 μ M MeJA lacked roots, so the percentile of wildtype and mutants that had an observable root was derived from the data. The data and associated graphical representation can be seen in Table 14 and Figure 22. Again, a significant effect on root growth is observed in the two KO lines, with the *AtST2b*- KO line being the most affected.

Table14: Percent of plants showing visible roots on day 3.

Ecotype	MS media (control)	MS+ 100 μ M MeJa
<i>Columbia 0</i>	100	67
<i>AtST2a-KO</i>	90	20
<i>AtST2b-KO</i>	92	8
<i>coi1-16</i>	100	100

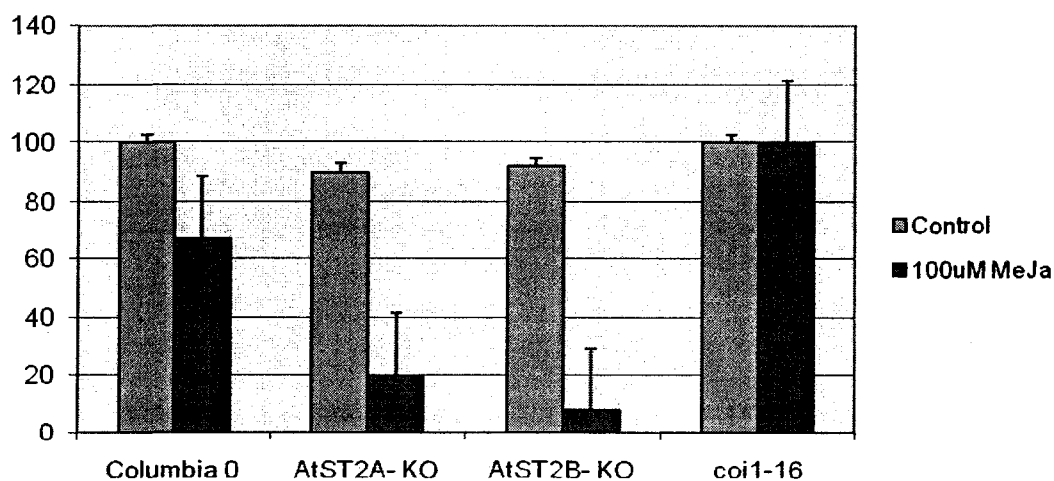


Figure 22: Percentage of plants with visible roots on day 3 (germination day) in wildtype and mutants on MS media as compared to MS +100 μ M MeJA.

3.4.3 Effect of different growth media on root length

Since jasmonates are known to have a growth inhibitory effect, you may recall that one possible role for AtST2a is to participate in the inactivation mechanism, where JA is transformed to 12-OHJA, which is in turn modified by the addition of the sulfonyl group. The roots of both the *AtST2a-KO* and *AtST2b-KO* lines are more severely affected in the presence of 100µM MeJA than the wildtype. *coi1-16* is, as expected, less sensitive to MeJA root inhibition (see Table 15). All genotypes behave the same in the control or 100 uM 12-OHJA experiments. These results indicate that 12-OHJA does not inhibit growth, as is the case with JA or MeJA, and that the function of AtST2a and AtST2b might be to participate in the inactivation of excess JA.

Table 15: Root length measurements of ten days old *coi1-16*, *AtST2a-KO*, *AtST2b-KO* and their wildtype background, Col0 on MS media, or media supplied with 100 uM MeJA or 100 uM 12-OHJA

Genotype	Control length (cm)	p Value	100uM MeJA (cm)	p Value	100uM 12-OHJA (cm)	p Value
Col0	7.0(±0.7)	-	1.1(±0.3)	-	6.8(±1.1)	-
Coi1	7.0 (±0.8)	1	3.9 (±1.2)	5.525-09	7.1 (±1.0)	0.4109
AtST2A KO	6.9 (±1.2)	0.7152	0.8 (±0.2)	0.0089	7.3 (±1.0)	0.2498
AtST2B KO	7.4 (±1.0)	0.2424	0.6 (±0.4)	0.0027	7.3 (±0.6)	0.1445

3.4.4 Effect of different photoperiod conditions on root growth

Light is known to inhibit root length growth in several plant species (Webb, 1983; Saugy *et al.*, 1989) and most *A. thaliana* studies link this process to an increase in ethylene levels. In view of the differential regulation of *Atst2a* and *AtST2b* in response to light and dark treatments (Levitin, 2004), and the knowledge that *AtST2a* is expressed in the root apical meristem and emerging lateral roots (Levitin, 2004), we investigated the effects of photoperiod on root length under continuous light or continuous dark, and compared it to wildtype grown plants. The *coi1-16* mutant, which is insensitive to the exogenous application of coronatine or JA, lacks the induction of *AtST2a* in the dark, suggesting an interaction between the photoperiod and JA pathways (Levitin, 2004). The *coi1-16* mutant was included as a plant which naturally lacks the ability to induce *AtST2a*, to compare with the *AtST2a*-deficient line. Roots of *AtST2a- KO*, *AtST2b- KO* and *coi1-16* grow significantly longer under continuous dark than does the *Col0* wildtype, but the differences disappear when placed back into light (see Table 15). All genotypes are significantly inhibited in their root growth under continuous light, but no difference is seen among genotypes. The results indicate that the an increase of internal 12-OHJA levels is not involved in the light-dependent control of root growth.

The experiment was conducted for two weeks, the first week, the plants were placed in one of the two conditions (continuous light or continuous dark), and the root length was measured. The following week, the plants were placed

into the opposite condition, i.e. if week 1 was continuous dark, the plants were placed under continuous light for the next week, and the opposite for the light grown plants. All differences among genotypes seemed to disappear or became insignificant in the second week, so the data for the second week was not included.

Exposing the plants to continuous light resulted in root inhibition that was consistent throughout the genotypes. In turn, exposing the plants to continuous dark also resulted in root inhibition that was stronger in the wildtype than it was in any of the JA mutant lines, with *AtST2b*-KO being again the least sensitive to dark. This draws another link between JA and the response to photoperiod.

Table 16: Root length measurements under different photoperiods of 7 days old *coi1-16 AtST2a-KO* and *AtST2b-KO* plants as compared to Col0.

Experiment	Length (cm) and probability value as compared to wild-type (Col0) (N=24)			
	Col0	<i>AtST2a-KO</i>	<i>AtST2b-KO</i>	<i>coi1-16</i>
LD (16h light 8h dark) Root	3.91	4.00	4.02	4.37
24h Light Root	2.83	2.97 (p= 0.322)	3.03 (p= 0.190)	2.92 (p= 0.543)
24h Dark Root	1.27	1.88 (p=0.003)	1.98 (p=0.001)	1.58 (p=0.026)
24h Dark Hypocotyl	1.921	1.800 (p=0.137)	1.731 (p=0.102)	1.958 (p=0.728)

3.4.5 Morphological studies

The studies on the histochemical distribution of *AtST2a* promoter fused to the GUS gene revealed very high levels of the gene in mature seeds, as well as dark-germinated, 2 days old seedlings (Figure 23) , and young seedlings placed in dark for 48h (Figure24) (Levitin, 2004). It was therefore of great interest to analyze the effect that a mutation in *AtST2a* would have on the plant at these various stages of development.

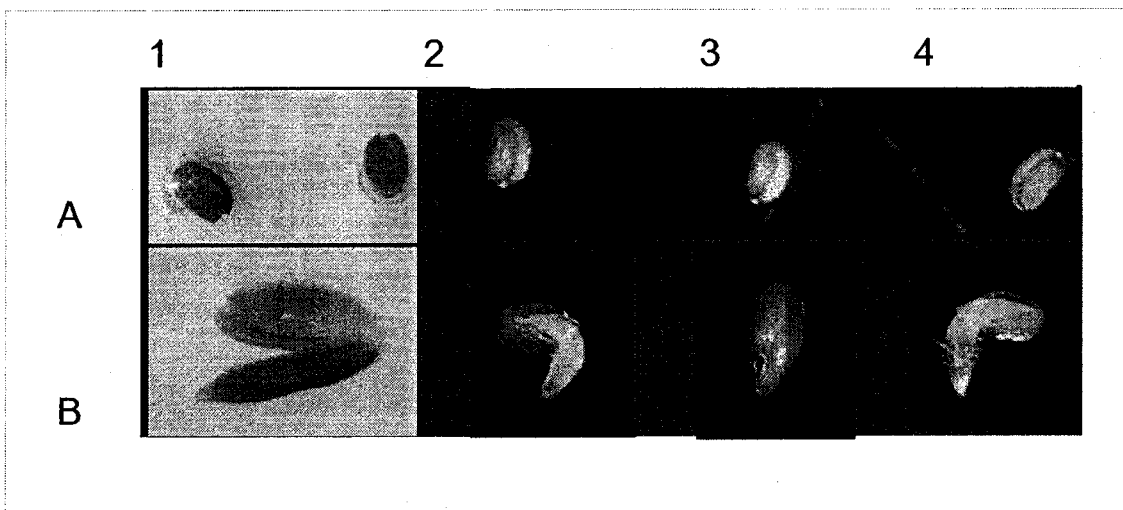


Figure 23: A) Seeds and B) 2 days old (dark-treated) seedlings of 1) GUS-*AtST2a* promoter transgenic plants, 2) Col0, 3) *AtST2a* -KO and 4) *AtST2b*-KO.

No phenotype was observed other than a possible increased sensitivity to dark of *AtST2a*-KO and decreased sensitivity to dark in *AtST2b*-KO (Figure 23b). A lengthier and more systematic study should be done to confirm this phenotype.

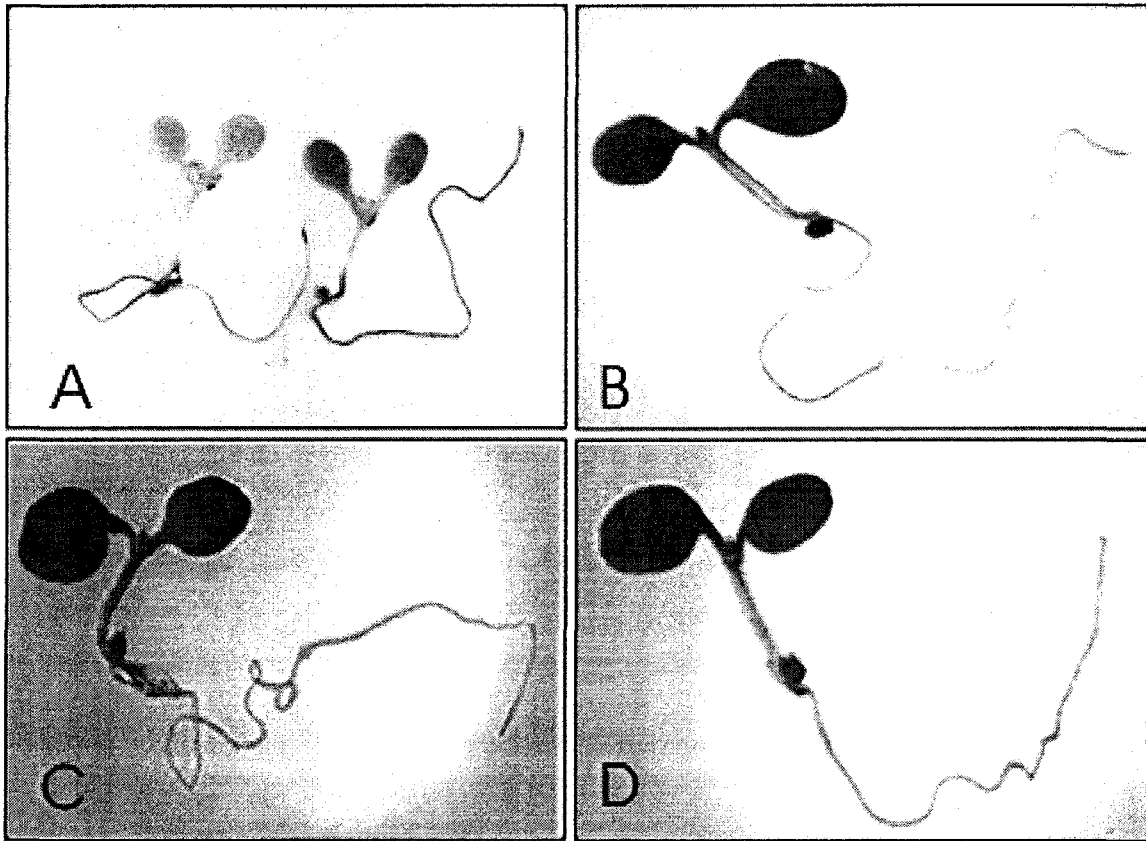


Figure 24: Twelve days old seedlings in A) GUS-*AtST2a* promoter transgenic plants, B) Col0, C) *AtST2a* -KO and D) *AtST2b*- KO, dark-treated for 48h

Jasmonates also influence flower development both by controlling pollen maturation and anther dehiscence, two uncoupled processes. This conclusion has been reached based on the phenotype of the male sterile OPDA-reductase 3 (*opr3*) mutant, which lacks the 12-oxophytodienoic acid reductase required for jasmonate synthesis. Its male sterile phenotype was shown to be rescued by the exogenous application of MeJA, but not OPDA (Stintzi and Browse, 2000). Additionally, it was shown that fertility could be restored by spraying the sterile flowers with 12-OHJA (Levitin, A, 2004).

Based on the knowledge that jasmonates are thus required for flower development, we wanted to investigate if an excess of 12-OHJA, as would be the case in the *AtST2a-KO* mutant, would also affect anther development. Careful flower dissection under the microscope confirmed that pollen maturation and anther dehiscence were not affected in either of the mutants (see Figure 25c), indicating that an excess of 12-OHJA has no effect on anther development. The role of 12-OHJA would have to be tested in a mutant lacking the enzyme that catalyzes the conversion of JA to 12-OHJA, but that enzyme is yet to be identified.

We also looked at organ development to see if differences were observed in the *AtST2a* and *AtST2b*- KO lines. However, no variance was seen in leaf, trichomes, lateral roots and root tips, or flower morphology between either of the three genotypes (Figure 25).

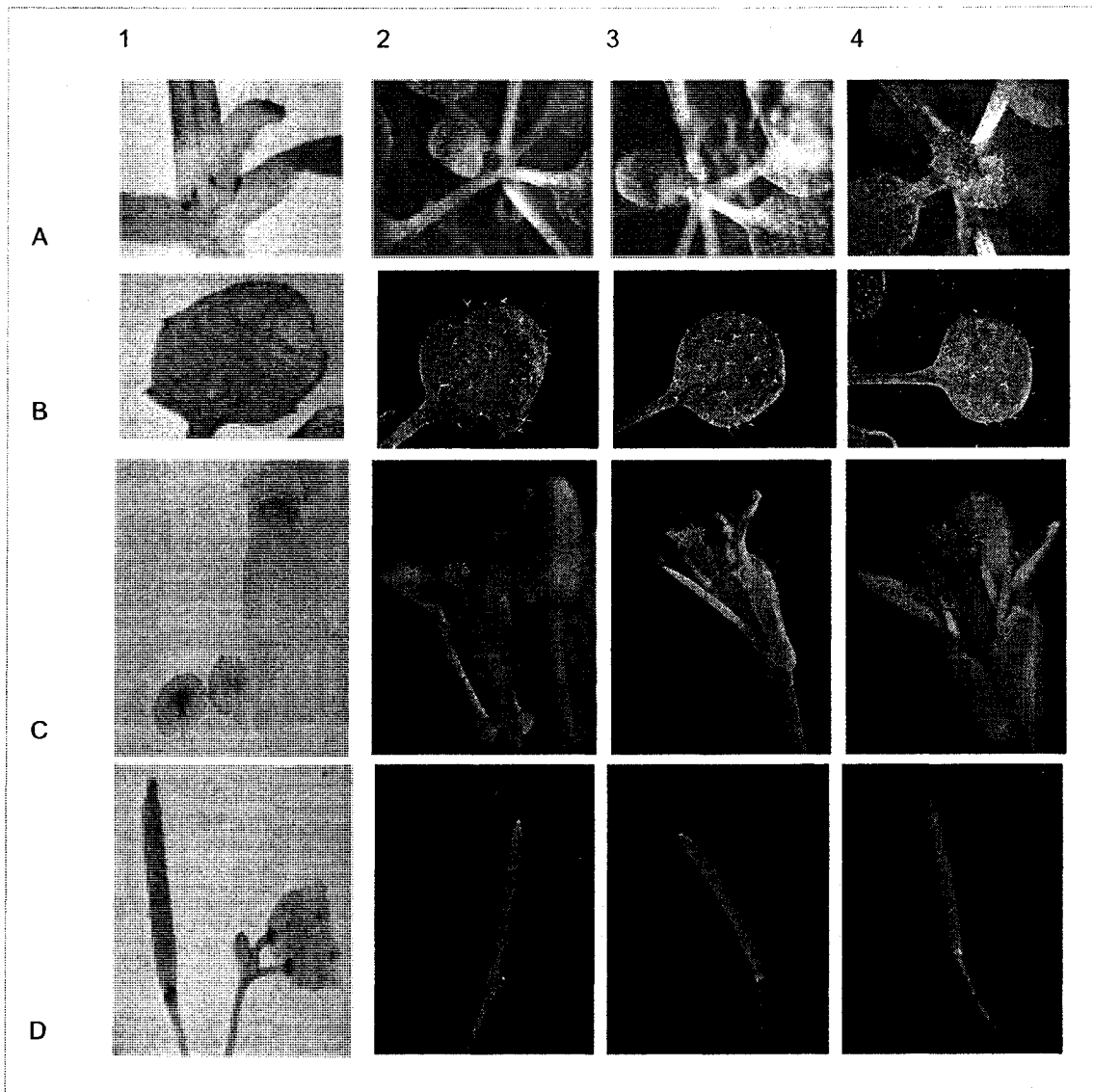


Figure 25: Mature A) apical meristem, B) leaves, C) flowers and D) siliques of 1) GUS-*AtST2a* promoter transgenic plants, 2) Col0, 3) *AtST2a* -KO and 4) *AtST2b*- KO.

3.4.6 Effect on Flowering Time

The next phenotype we wanted to investigate was the flowering time and developmental stage at flowering time (based on total leaf number) of the two KO lines under different photoperiods. 12-OHJA has been previously shown to have tuber-inducing properties in *Solanum tuberosum*. If we transpose this to our model organism, the accumulation of 12-OHJA in the floral meristem suggests that it might play a role in the vegetative to floral transition, if we assume that the end process affected lies in the generation of offspring. Indeed, previous flowering time analyses on sense and antisense lines showed differential photoperiod-dependent timing: under LD, sense lines flower later than wildtype, while under SD antisense lines flower early compared to the wildtype. We therefore decided to study the effect of knocking out the *AtST2a* or the *AtST2b* gene on *A. thaliana* flowering time under both long and short day conditions. Thirty-two plants each of Col0, *AtST2a-KO* and *AtST2b-KO* were grown for each of the two experiments and monitored daily for the appearance of the first flower bud. When this was seen, the day and total leaf number was noted, and the averages used to evaluate flowering time and growth stage.

3.4.6.1 Long Day Analysis

RT-PCR results show that *AtST2a* is normally not expressed under inductive (LD) photoperiod, pointing towards a requirement of 12-OHJA in the flowering process. Based on this, we do not expect the mutant lines to act any different than the wildtype under these conditions. Indeed, the average (n=30) flowering time varies only minutely, from 19.7 days in wildtype, to 20.1 and 20.8 days in the *AtST2a-KO* and *AtST2b-KO* lines respectively, and the plants seem to be in the same developmental stage at the onset of flowering, based on the total number of leaves (see Table 17).

Table 17: Number of days to the first flower and total leaf number for Col0, *AtST2a*- KO and *AtST2b*- KO under long day conditions

Genotype (N=30)	# Days to first flower	p Value	# leaves upon first flower	p Value
Col0	19.7 (± 2.4)	-	11.6 (± 1.1)	
<i>AtST2A</i> KO	21.1 (± 2.9)	0.4130	10.9 (± 1.2)	0.2400
<i>AtST2B</i> KO	21.8 (± 2.8)	0.1908	10.4 (± 1.6)	0.1803

3.4.6.2 Short Day Analysis

Although not normally expressed under LD conditions, *AtST2a* is induced upon exposure to dark for longer than 8 consecutive hours (Levitin, A. 2004). In contrast, *AtST2b* is known to be slightly repressed by dark (Genevestigator: ctrl/dark ratio=0.77) Previous flowering time studies using antisense *AtST2a* lines showed the mutant to flower significantly earlier only under SD conditions. Contrary to what we would have expected, in the current experiment, only the *AtST2b*- KO shows an altered phenotype in both flowering early at 50 days

compared to 56 days for the wildtype and having more leaves upon flowering (see Table 18). The contradictory results seen in the antisense line and the knockout lines are most likely a consequence of the antisense line still having the sulfated form of 12-OHJA.

Table 18: Number of days to the first flower and total leaf number for Col0, AtST2A KO and AtST2B KO under short day conditions

Genotype (N=30)	# Days to first flower	p Value	# leaves upon first flower	p Value
Col0	56.3(±2.5)	-	41.6 (±2.7)	
AtST2A KO	55.1 (±4.0)	0.3540	41.9 (±4.0)	0.6938
AtST2B KO	50.2(±3.7)	1.234E-11	43.3 (±3.7)	3.647E-02

Together, the number of leaves upon flowering and flowering time analysis indicate that at the same age, *AtST2b-KO* is in a later stage of development than its wildtype counterpart or the *AtST2a-KO* in SD conditions.

3.4.7 Seed production

Finally, based on the high levels of GUS stain seen in mature seeds of plants whose *AtST2a* promoter was linked to the GUS reporter gene, fertility was further tested in terms of seed production (see Table18). No significant difference in seed number was observed between the genotypes. The experiment was conducted only under LD growth conditions, so further investigation is needed to confirm that no phenotype is visible under SD as well.

Table 19: Seed production in terms of number of seeds per silique of mature (45 days old) plants.

Ecotype	# seeds/ silique
Col0	32.3
AtST2a KO	32.7 (p= 0.724)
AtST2b KO	35.1 (p= 0.227)

4.0 Discussion

Sulfotransferases are enzymes with highly conserved structures present in all organisms studied to date, from prokaryotes to eukaryotes. This high level of conservation throughout organisms and across kingdoms indicates a crucial role for the reaction they catalyze. These reactions have been shown to range in function from the inactivation of bioactive metabolites (such as hormones, small drugs and xenobiotics), to, the activation of compounds such as prodrugs, procarcinogens or some neuropeptide hormones (Falany, 1997a, b, Duanmu *et al*, 2001). With few exceptions, sulfotransferases tend to be highly specific in their substrate preference.

Compared with the large body of information available on animal sulfotransferases, little is known regarding their function in plants. The availability of the genome sequence of *A. thaliana* makes it the model of choice to initiate a functional analysis of the sulfotransferases present in a flowering plant. The 18 sulfotransferases present in the *A. thaliana* genome have been grouped into 10 families based on their amino acid sequence alignment. Of these, AtSt2a has been shown to sulfonate specifically 11- and 12-hydroxyjasmonic acid with a higher affinity for the latter (Levitin, A., 2004). Its homolog, AtSt2b, the only other member of the AtST2 family, did not show any enzymatic activity in the presence of these jasmonates. Despite considerable efforts, previous studies did not define the substrate preference of this enzyme.

AtST2a expression was shown to be regulated by the light perception pathway. Significant mRNA and protein levels were only detected when the

plants were exposed to a period of dark lasting at least 8h (Levitin, 2004). *AtST2a* expression is also induced by the exogenous application of 12-OHJA and MeJA (Levitin, 2004). Localization studies using an *ATST2a*promoter::*GUS* fusion have shown expression in seedlings, young developing leaves, shoot and root apical meristem, flower organs and at the base of siliques (Levitin, A., 2004). Transgenic plants carrying an additional copy of *AtST2a* in the sense or antisense orientation were shown to be affected in their flowering time. Plants overexpressing *AtST2a* in the sense orientation under the CaMV 35S constitutive promoter flower later than wildtype in flower-inducing conditions (i.e. long days), while plants carrying *AtST2a* in the antisense orientation flowered earlier than wildtype in flowering repressive conditions (i.e. short days) (Levitin, A., 2004). The results of these functional studies point toward an important role for 12-OHJA in the control of flowering time and suggest that its biological activity is modulated by the sulfonation reaction catalyzed by *AtST2a*. However, other experimental evidences suggest that 12-OHJA might simply be an intermediate in the catabolism of excess jasmonic acid and that the sulfonation reaction is just another step in the inactivation mechanism.

In agreement with this latter hypothesis, studies of the uptake and metabolism of JA and MeJA in tobacco BY2 cells have shown that 11- and 12-OHJA were the preferential metabolites excreted in the medium, followed by glycosyl esters of hydroxyjasmonates (Swiatek *et al*, 2004). The levels of the hydroxylated and glycosylated metabolites in the cell extracts were below detection limit. These results suggest the presence in plant cells of an active

mechanism that deals with excess JA by its excretion following hydroxylation and glycosylation. Unfortunately, in this experiment the researchers did not quantify specifically the levels of 11- or 12-OHJA-SO₄ in the cell extracts and in the growth medium making it impossible to confirm that the sulfonation reaction catalyzed by AtST2a is part of this excretion pathway.

In light of the seemingly contradictory evidences available so far, we decided to investigate in more detail the function of 12-OHJA and determine if it has an intrinsic biological activity, or if it is only an intermediate in the catabolism of JA. To conduct these studies we used two approaches. First, we performed microarray experiments on plants treated with MeJA or 12-OHJA to determine if 12-OHJA regulates its own subset of genes. Second, we took advantage of available T-DNA insertion mutant lines in the *AtST2a* gene to investigate the effect on growth and development of a reduction in the endogenous level of 12-OHJA sulfate. We also included in the latter analyzes a T-DNA insertion line in the *AtST2b* gene to try to define its biochemical and biological function.

4.1 12-OHJA has a biological role, independent of MeJA

To find out if 12-OHJA has a biological activity independent from MeJA, mRNA extracted from untreated plants or plants treated with either compound were subjected to microarray analysis. The experiment was carried out on the Affymetrix GeneChip ATH22K array, which contains probes for nearly all protein-coding genes of Arabidopsis. Four hours following treatment, 1763 transcripts

met our criteria for differential expression (displaying ratios ≥ 1.5 -fold induction and ≤ 0.5 -fold repression).

Figure 8 shows that 45 genes are induced and 7 genes are repressed exclusively in response to 12-OHJA treatment (clusters 1 and 6). The small number of genes present in these clusters as compared to the ones regulated by MeJA alone, or by MeJA and 12-OHJA (which range in the hundreds of genes) may be due to a more restricted function of 12-OHJA as compared with MeJA, or to higher concentrations or time of treatment required for a more robust effect of 12-OHJA on gene expression. It is important to note that the addition of an hydroxyl group on JA reduces its diffusion through membranes. Because of this difference in the solubility and permeability of the two molecules, a direct comparison of the effect on gene expression at the same concentration cannot be made. The identification of genes responding exclusively to MeJA or to 12-OHJA indicates the presence of separate pathways responding to these molecules and suggests that the two molecules have different functions in *A. thaliana*. To better understand the function of 12-OHJA, it would be interesting to study the impact on growth, development and adaptation to stress of a loss of function mutation in the enzyme that hydroxylates JA to 12-OHJA. Efforts are underway for identifying such gene, directed by the data from the microarray experiment (Kappert, T.L., personal communication).

To validate our data, we compared our results with the ones reported in the literature for genes that are known to be regulated by MeJa (Zimmermann *et al*, 2004). The results presented in tables 9 and 10 confirm the validity of our

results, as the selected genes show patterns similar to what is reported in the literature. For example, genes in the response to wounding such as *vegetative storage protein (VSP)*, the defense response genes *thionin 2.1 (Thi2.1)* and the *plant defensin gene 1.2 (Pdf1.2)*, other known regulated genes such as chlorophyllase (*CLH*), myrosinase-binding protein (*MBP*) or genes of the JA biosynthetic pathway (*LOX*, *OPR*, *AOS*, *AOC*) are all induced in our experiments, (table 9), while genes involved in photosynthesis and carbohydrate assimilation, as well as transcription factors are generally repressed (table 10).

We further compared the results of the microarray experiments to those obtained by RT-PCR and found that the profiles were consistent. The level of expression of our two SULTs of interest, the marker gene *Thi2.1*, as well as 6 other randomly selected genes from different clusters was tested by RT-PCR. The results were then compared to the intensity values from the microarray data, which are presented in table 10. When comparing those values to the intensity of the fragments amplified by PCR presented in figure 9, we see that similar results are obtained with both experiments.

As reported earlier in the literature, MeJA induces genes in signal transduction pathways and hormone responsive categories, and slightly those involved in biotic and abiotic responses (figure 10 A). In turn, it represses transporters and genes involved in energy production, and slightly represses developmental genes as well as genes in the protein and plant metabolism categories (figure 10 B), while an equal number of transcription factors are induced or repressed by MeJA. 12-OHJA also induces genes involved in signal

transduction, as well as genes in the biotic and abiotic response pathway (figure 11 A), while the most drastic repression is seen in transporters, followed by genes encoding proteins involved in hormone response and development (figure 11 B). A relatively limited number of genes are present in the clusters representing genes responding only to 12-OHJA making it difficult to extract meaningful information as to the processes that are mostly affected by the exogenous application of 12-OHJA. Taken together, the results suggest the presence of individual pathways responding to MeJA and 12-OHJA and of a pathway responding to both molecules. The significance of the overlapping (figure 12) and unique (figures 10 and 11) functions of each compound remains to be characterized. To be able to address specifically this question, the characterization of a loss of function mutant unable to convert JA into 12-OHJA is required.

4.2 Expression of JA- biosynthesis genes in *AtST2a*- and *AtSt2b*-KO plants

It has been shown previously that the modulation of the endogenous levels of JA has an effect on the expression of genes involved in its biosynthesis (Creelman and Mullet, 1997). Furthermore, it has been shown that the expression of these genes is repressed in the dark (Zimmermann *et al*, 2004). In contrast, *AtST2a* was shown to be induced in the dark (Levitin, A., 2004). According to its biochemical function, we can predict that the *AtST2a*-KO plant might have increased accumulation of 12-OHJA and we have shown a drastic

decrease in the accumulation of its sulfonated derivative (Gidda *et al*, 2003). We wanted to test if the accumulation of abnormal levels of the two metabolites *in vivo* has an impact on the expression of genes involved in JA biosynthesis. The *protochlorophyllide oxidoreductase A (PORA)* gene was used in this study to ensure that the mutants were not affected in their response to dark.

The results of figure 15 show that the light-dependent expression of *PORA* is not affected in the *AtST2a*- and *AtST2b*-KO plants, being repressed by dark in both mutants. The jasmonic acid biosynthesis pathway genes *AOS*, *AOC4* and *OPR3*, are expressed in the light and repressed in the dark in wildtype plants (Zimmermann *et al*, 2004). The same pattern is observed in the *AtST2a*- and *AtST2b*-KO, as well as the *coi1-16* mutant. Assuming that the intensities of the bands reflect accurate mRNA levels, it seems that the *AtST2b*-KO compensates by producing more *AtST2a* under control conditions than a wildtype plant, and the same is true for the *AtST2b* gene in the *AtST2a*-KO background. Furthermore, genes in the JA-pathway seem to be upregulated in both *AtST2a*- and *AtST2b*-KOs as compared to wildtype plants. Quantification of the levels of JA and 12-OHJA in mutant and wildtype plants will be required to understand the basis of this deregulation of JA biosynthetic genes in the mutants.

4.3 The function of *AtST2a* is to sulfonate 12-OHJA and is disrupted in the *AtST2a*-KO mutant

12-OHJASO₄ was shown to elute on HPLC between fractions 29 and 31 (figure 16). These fractions were thus collected from metabolite extracts from

wildtype, *AtST2a*- and *AtST2b*-KO plants, and verified for the presence of 12-OHJASO₄ by mass spectrometry. The profiles seen in figure 17 show the presence of an ion with a mass of 305 [M-1], corresponding to the predicted mass of 12-OHJASO₄ in the negative mode (Gidda *et al*, 2003). The identity of this molecule was further confirmed by MS/MS by comparison with authentic 12-OHJA (figure 18). This ion is also present in the extract from an *AtST2b*-KO plant indicating that *AtST2b* is not involved in the sulfonation of 12-OHJA *in-vivo*. As expected, the ion is absent from the *AtST2a*-KO extract. The data therefore confirms the results of *in-vitro* studies and indicate that *AtST2a* is catalyzing the sulfonation of 12-OHJA *in-vivo*. Furthermore, the results indicate that the other member of the *AtST2* family, *AtST2b*, does not have the same biochemical function.

The figure also shows the presence of another more abundant ion with a mass of 307 [M-1]. Further investigation of the fragmentation pattern of this metabolite shows that some fragments are identical to those of 12-OHJASO₄, while others contain an additional mass of two daltons, corresponding to the loss of the double bond in the side chain of 12-OHJASO₄ (Figure 19 right). It is the first time that this jasmonate is reported to occur in plants. The presence of this highly related compound in our profiles gives rise to an interesting question: Which sulfotransferase of *Arabidopsis* is involved in its synthesis? When we consider the high level of structural similarity between the two metabolites and the two enzymes, we can hypothesize that both *AtST2a* and *AtST2b* are involved in the sulfonation of this new metabolite while *AtST2a* would be the only enzyme

able to sulfonate 12-OHJA. A careful examination of the mass spectra reveals that the ratio between the relative abundance of the 305 and 307 ions increases when we compare *AtST2b*-KO and wildtype plants suggesting that the synthesis of the 307 ion is decreased in the mutant. In the future, we will purify this compound and assay its desulfated derivative with recombinant *AtST2a* and *AtST2b* enzymes to confirm this hypothesis.

4.4 Decreased internal levels of 12-OHJASO₄ do not give rise to a visible phenotype in the *AtST2a*-KO line

Phenotypic analysis of *AtST2a* and *AtST2b* loss of function mutants was performed at different growth stages. This analysis was performed to try to define their biological function. Unfortunately, the tight linkage between the two genes did not allow the production of the double mutant by genetic crosses.

Germination

Histochemical studies using the GUS gene linked to the *AtST2a* promoter showed high expression in mature seeds (Levitin, A. 2004). To find out if seed maturation was affected in the two mutants, we investigated the germination time and viability of *AtST2a*- and *AtST2b*-KO seeds. The results show that the two mutants were not affected in their germination time (Table 12) or in the germination percentile (Table 13). We also quantified the number of siliques and seeds per silique for the two mutants and compared it to wildtype plants. The results show no significant difference between the different lines (Table 19).

Despite high level of expression in mature siliques, the function of *AtST2a* and *AtST2b* does not seem to be linked to seed yield.

In view of a possible role of 12-OHJA and its sulfated derivative in the inactivation of excess JA, we analyzed germination time and percentile of the two mutants when grown in presence of MeJA. If indeed *AtST2a* or *AtST2b* are involved in a detoxification process, we would expect the mutants to be more sensitive to the exogenous presence of MeJA. The MeJa insensitive *coi1-16* mutant was included as a control since it should not be affected by the presence of MeJA in the growth media (Feys *et al*, 1994). As expected, the percent germination of the *coi1-16* mutant is always 100% regardless of the medium tested (see table 13). Interestingly, the *AtST2b*-KO mutant, which was not expected to show a phenotype in the presence of MeJA, since the gene is not induced by the hormone, is more affected than *AtST2a*-KO and wildtype plants. Furthermore, whereas both wild type and *coi1-16* mutant plants have clearly visible roots after germination, none or fewer roots are visible in both *AtST2a*- and *AtST2b*-KO seedlings. These results suggest that *AtST2a* and *AtST2b* might participate in a pathway that eliminates excess JA. The fact that the *AtST2b*-KO line exhibits the strongest phenotype suggests that its role is crucial in this process. Unfortunately, since we do not know exactly the biochemical function of this enzyme, it is difficult to explain the reason for the increased sensitivity of this mutant to exogenous JA. However, the results suggest that *AtST2b* might be involved in the sulfonation of a jasmonate derivative.

Root growth

Based on previous results showing high level of expression of *AtSt2a* in root apical meristem and emerging lateral roots, we studied root growth in this mutant. We also studied the effect on root growth of a loss of function mutation in *AtST2b*. The analyses were done under different light regimes which are known to affect the expression of *AtST2a*.

Continuous light consistently reduces the root length in all genotypes, but no significant difference is seen when we compare the two mutants and wildtype plants. On the other hand, under continuous dark the roots of *AtST2a*-KO, *AtST2b*-KO and *coi1-16* mutant plants grow, to different extent, longer than the wild type ones. The results suggest that the sulfonation of jasmonates is involved in root growth inhibition in the dark. It is important to note that in wildtype plants only *AtST2a* expression is induced in the dark suggesting that the sulfonation of 12-OHJA plays a role in the control of root growth and that this control is modulated by photoperiod. However, the results presented in table 15 demonstrate that the exogenous application of 12-OHJA has no effect on root growth suggesting that the effect that we observe cannot be explained by the increased accumulation of 12-OHJA in the *AtST2a*-KO plants. It is possible that the inhibitory effect is due to the accumulation of 12-OHJASO₄ in the dark or by another uncharacterized sulfonated jasmonate. To test this hypothesis, we will have to quantify the different jasmonates and their sulfonated derivatives under different light regimes and try to relate their relative abundance with the growth behaviour of the plants.

Flowering time

In order to position *AtST2a* and *AtST2b* in the pathways controlling flowering initiation, their expression pattern in wild type and dark treated plants was determined in the light perception mutants *toc1* and *co*, and in the autonomous pathway mutants *fca1* and *fca2*.

The expression of *AtST2a* is no longer induced in the dark in a *co* mutant, indicating that it is downstream of CO in the photoperiod promotion pathway (Figure 14). The fact that *AtST2a* expression is still induced in the dark in a *fca* mutant suggests that it is positioned upstream of the point where the temperature pathway (*fca*) meets the photoperiod pathway (*co*) (Figure 2). As expected, the expression of *AtST2a* is no longer induced in the dark in the *toc1* mutant, as this gene is situated upstream of *co* in the photoperiod pathway. In contrast, the expression of *AtST2b* is unaffected in a *co* mutant background, but seems to be induced by dark treatment in a *toc* mutant. This result is unexpected, since *TOC 1* is known to be upstream of CO in the photoperiod pathway (Blazquez et al, 2000). It also seems that the expression of *AtST2b* is reversed in an *fca-1* mutant, and disappears entirely in a *fca-2* mutant. These results suggest that the expression of *AtST2b* is regulated by the autonomous pathway downstream of *FCA*. Although some results are inconsistent with what is expected based on the known position of genes in the flower development pathway, they have been confirmed by RT-PCR multiple times and were always consistent. To clarify this situation, further studies using other mutants in the light perception pathway such as *tfl2*, and in the autonomous pathway such as *flic* and *lfy* might prove more

useful to position the *AtST2b* gene in the photoperiod and in the autonomous pathway.

The flowering time experiments were carried out under both LD and SD photoperiods. The total leaf number at the time of flowering was also recorded to compare the developmental stage of the plants when the inflorescence emerges from the rosettes. Based on the fact that the *AtST2a* mRNA level seems to increase only after 8h of dark exposure, the effect on flowering of the accumulation of higher 12-OHJA level in the *AtST2a*-KO mutant is expected to be more apparent, if any, in SD grown plants.

In fact, what tables 17 and 18 show is exactly this, but not for the line we expected. Flowering time and development stage at the time of flowering is unaffected in any of the KO lines as compared to the wild type under a long day photoperiod (table 17). Under short days though, it is the *AtST2b*-KO, not the *AtST2a*-KO that shows an altered flowering time (table 18). Furthermore, it also has approximately 2 more leaves than wild type at the time of flowering indicating that growth is accelerated in this mutant. It is surprising to see that the loss of *AtST2a* has almost no impact on flowering time since this gene is regulated by the photoperiod promotion pathway. In view of the relatively mild effect on flowering time of the mutation in *AtST2a* and *AtST2b*, it is difficult to assign a function for these genes in this flower initiation. The subtle phenotype of the individual mutants could be due to the fact that the two genes might have a partially redundant function. The construction of the *AtST2a* and *AtST2b* double

mutant will be required to find out if these genes are really playing an important function in the control of flowering time.

Other morphological Analysis

The results of previous studies conducted with the *GUS* protein expressed under the control of the *AtST2a* promoter were used to focus on specific tissues or organs during our morphological observations under the microscope. Unfortunately, and despite numerous attempts, we did not observe any modification of the plant morphology at any of the investigated sites.

5.0 Concluding Remarks and Future Work

Our results indicate that plants respond specifically to 12-OHJA by inducing or repressing the expression of a small number of genes. Unfortunately, the function of these genes has not been characterized making it difficult to predict the function of this metabolite in the growth or development of the plants. Furthermore, some of the results suggest that the only function of *AtST2a* and *AtST2b* is to cope with an excess of JA. More studies will be required to better understand the function of these genes.

In the future, we will concentrate our efforts on:

- The characterization of the biochemical function of *AtST2b*
- The construction of the *AtST2a* and *AtST2b* double mutant line using RNA interference (RNAi).

The availability of the double mutant will allow us to find out if the two enzymes have redundant function *in vivo* by comparing their sulfonated metabolomes. In addition, phenotypic analyses of the double mutant should clarify the function of these genes in root growth and in the control of flowering time.

References:

- Alvarez, J., Guli, C. L., Yu, X-H. and Smyth, D. R. (1992). TERMINAL FLOWER: a gene affecting inflorescence development in *Arabidopsis thaliana*. *Plant J.* 2, 103-116.
- Arabidopsis* Genome Initiative. 2000. Analysis of the genome sequence of the flowering plant *Arabidopsis thaliana*. *Nature* 408: 796-815
- ABRC (Arabidopsis Biological Resource Center) available through The Arabidopsis Information Resource (TAIR), at http://www.arabidopsis.org/abrc/acquis_deacquis.jsp on <http://www.arabidopsis.org>.
- Baumann, E. (1876). Ueber sulfosauren im harn. *Dtsch. Chem. Ges.* 54–58.
- Becker, W., and Apel, K. (1992). Isolation and characterization of a cDNA clone encoding a novel jasmonate-induced protein of barley (*Hordeum vulgare* L.). *Plant Mol Biol* 19, 1065-1067.
- Bernier, G., and Perilleux, C. (2005). A physiological overview of the genetics of flowering time control. *Plant Biotechnol J* 3, 3-16.
- Bernier, G. (1988). The control of floral evocation and morphogenesis. *Annu. Rev. Plant Physiol. Plant Mol. Biol.* 39, 175–219.
- Blazquez, M. (2000). Flower development pathways. *J Cell Sci* 113 (Pt 20), 3547-3548.
- Blechert S, Bockelmann C, Fusslein M, Von Schrader T, Stelmach B, Niesel U, Weiler EW (1999) Structure-activity analyses reveal the existence of two separate groups of active octadecanoids in elicitation of the tendril-coiling response of *Bryonia dioica* Jacq. *Planta* 207: 470–479.
- Campbell and Reece. *Biology*. 5th edition. Pearson Education, Inc., publishing as Benjamin Cummings. 1999.
- Cohen Y., Gisi, U., Niderman, T. 1993. Local and systemic protection against *Phytophthora infestans* induced in potato and tomato plants by jasmonic acid and jasmonic methyl ester. *Phytopathology*. 83, 1054-1062
- Corbesier, L., and Coupland, G. (2006). The quest for florigen: a review of recent progress. *J Exp Bot* 57, 3395-3403.

- Corbesier L., Kustermans G., Périlleux C., Melzer S., Moritz T., Havelange A. & Bernier G. (2004) Gibberellins and the floral transition in *Sinapis alba*. *Physiologia Plantarum* 122, 152–158.
- Corbineau, F., R.M. Rudnicki, D. Come, 1988. The effects of methyl jasmonate on sunflower (*Helianthus annuus* L.) seed germination and seedling development. *Plant Growth Regul.*, 7, 157-169.
- Creelman, R.A., and Mullet, J.E. (1997). Biosynthesis and Action of Jasmonates in Plants. *Annu Rev Plant Physiol Plant Mol Biol* 48, 355-381.
- Creelman, R.A., Tierney, M.L., and Mullet, J.E. (1992). Jasmonic acid/methyl jasmonate accumulate in wounded soybean hypocotyls and modulate wound gene expression. *Proc Natl Acad Sci U S A* 89, 4938-4941.
- Daletskaya TV, Sembdner G (1989) Effect of jasmonic acid. on germination of nondormant and dormant seeds (russ.). *Fisiol rast* 36: 1118-1123
- Deng W, Hamilton-Kemp TR, Nielsen MT, Andersen RA, Collins GB, Hildebrand DF. 1993. Effects of six-carbon aldehydes and alcohols on bacterial proliferation. *J. Agric. Food Chem.* 41: 506– 10
- Duanmu, Z., Kocarek, T.A., and Runge-Morris, M. (2001). Transcriptional regulation of rat hepatic aryl sulfotransferase (SULT1A1) gene expression by glucocorticoids. *Drug Metab Dispos* 29, 1130-1135.
- Falany, C.N. (1997a). Sulfation and sulfotransferases. Introduction: changing view of sulfation and the cytosolic sulfotransferases. *Faseb J* 11, 1-2.
- Falany, C.N. (1997b). Enzymology of human cytosolic sulfotransferases. *Faseb J* 11, 206-216.
- Farmer, E.E., and Ryan, C.A. (1992). Octadecanoid Precursors of Jasmonic Acid Activate the Synthesis of Wound-Inducible Proteinase Inhibitors. *Plant Cell* 4, 129-134.
- Feys, B., Bendetti, CE, Penfold C.N., and Turner, J.G. (1994). Arabidopsis Mutants Selected for Resistance to the Phytotoxin Coronatine Are Male Sterile, Insensitive to Methyl Jasmonate, and Resistant to a Bacterial Pathogen. *Plant Cell*, 6(5):751-759.
- Finch-Savage, W.E., Blake, P.S., Clay H.A. (1996). Desiccation stress in recalcitrant *Quercus robur* L. seeds results in lipid peroxidation and increased synthesis of jasmonates and abscisic acid *Journal of Experimental Botany.* 47, 661-667

- Gidda, S.K. (2001). Molecular and Biochemicam characterization of hydroxyjasmonate and flavonoid sulfotransferases from *Arabidopsis thaliana*. Concordia, Montreal.
- Gidda, S.K., Miersch, O., Levitin, A., Schmidt, J., Wasternack, C., and Varin, L. (2003). Biochemical and molecular characterization of a hydroxyjasmonate sulfotransferase from *Arabidopsis thaliana*. *J Biol Chem* 278, 17895-17900.
- Gundlach, H., M. J. Muller, T. Kutchan, M. H. Zenk, 1992. Jasmonic acid is a signal transducerin elicitor-induced plant cell cultures. *Proc. Natl. Acad. Sci. USA*, 89,2389–2393.
- Hamberg, M., and Fahlstadius, P. (1990). Allene oxide cyclase: a new enzyme in plant lipid metabolism. *Arch Biochem Biophys* 276, 518-526.
- Hamberg M, Hughes MA. Fatty acid allene oxides. III. Albumin-induced cyclization of 12,13(S)-epoxy-9(Z),11-octadecadienoic acid. *Lipids*. 1988; 23:469–475.
- Hildebrand, D.;Fukushige, H.;Afitlhile, M.; Wang, C. Lipoxygenases in plant development and senescence. In: Rowley A, Kuhn H, Schewe T. , editors. *Eicosanoids and Related Compounds in Plants and Animals*. London: Portland Press Ltd.; 1998. pp. 151–181.
- Howe, G.A. (2001). Cyclopentenone signals for plant defense: remodeling the jasmonic acid response. *Proc Natl Acad Sci U S A* 98, 12317-12319.
- Howe, G.A., Lightner, J., Browse, J., and Ryan, C.A. (1996). An octadecanoid pathway mutant (JL5) of tomato is compromised in signaling for defense against insect attack. *Plant Cell* 8, 2067-2077.
- Irizarry, R.A., Hobbs, B., Collin, F. Beazer-Barclay, Y. D., Antonellis, K. J. Scherf, U. and Speed T. P. (2003). Exploration, normalization, and summaries of high density oligonucleotide array probe level data. *Biostatistics*. v4. 249-264.
- Ishikawa, A., Yoshihara, T., and Nakamura, K. (1994). Jasmonate-inducible expression of a potato cathepsin D inhibitor-GUS gene fusion in tobacco cells. *Plant Mol Biol* 26, 403-414.
- Ishiguro S, Kawai-Oda A, Ueda J, Nishida I, Okada K (2001) The Defective in Anther Dehiscence1 gene encodes a novel phospholipase A1 catalyzing the initial step of jasmonic acid biosynthesis, which synchronizes pollen maturation, anther dehiscence, and flower opening in *Arabidopsis*. *Plant Cell* 13: 2191–2209

- Johnson, R., Narvaez, J., An, G., and Ryan, C. (1989). Expression of proteinase inhibitors I and II in transgenic tobacco plants: effects on natural defense against *Manduca sexta* larvae. *Proc Natl Acad Sci U S A* 86, 9871-9875.
- King, K.E., Moritz, T., and Harberd, N.P. (2001). Gibberellins are not required for normal stem growth in *Arabidopsis thaliana* in the absence of GAI and RGA. *Genetics* 159, 767-776.
- King, R.W., and Zeevaart, J.A. (1973). Floral Stimulus Movement in *Perilla* and Flower Inhibition Caused by Noninduced Leaves. *Plant Physiol* 51, 727-738.
- King, R.W., Evans, L.T., and Wardlaw, I.F. (1968). Translocation of the floral stimulus in *Pharbitis nil* in relation to that of assimilates. *Z. Pflanzenphysiol.* 59, 377-388.
- Klaassen, C.D., and Boles, J.W. (1997). Sulfation and sulfotransferases 5: the importance of 3'-phosphoadenosine 5'-phosphosulfate (PAPS) in the regulation of sulfation. *Faseb J* 11, 404-418.
- Klein, M., and Papenbrock, J. (2004). The multi-protein family of *Arabidopsis* sulphotransferases and their relatives in other plant species. *J Exp Bot* 55, 1809-1820.
- Koda Y, Kikuta Y, Tazaki H, Tsujino Y, Sakamura S, Yoshihara T (1991) Potato tuber-inducing activities of jasmonic acid and related-compounds. *Phytochemistry* 30: 1435-1438.
- Koda, Y. (1992). The role of jasmonic acid and related compounds in the regulation of plant development. *Int Rev Cytol* 135, 155-199.
- Lang, A., Chailakhyan, M.K., and Frolova, I.A. (1977). Promotion and inhibition of flower formation in a dayneutral plant in grafts with a short-day plant and a long-day plant. *Proc Natl Acad Sci U S A* 74, 2412-2416.
- Levitin, A. (2004). Molecular and biochemical characterization of two of *Arabidopsis thaliana* sulfotransferases: AtST2a and AtST2b. PhD thesis. Concordia University, Montreal.
- Levy, Y.Y., and Dean, C. (1998). Control of flowering time. *Curr Opin Plant Biol* 1, 49-54.
- Macknight, R., Duroux, M., Laurie, R., Dijkwel, P., Simpson, G., and Dean, C. (2002). Functional significance of the alternative transcript processing of the *Arabidopsis* floral promoter FCA. *Plant Cell* 14, 877-888.

- Macknight, R., Bancroft, I., Page, T., Lister, C., Schmidt, R., Love, K., Westphal, L., Murphy, G., Sherson, S., Cobbett, C., and Dean, C. (1997). FCA, a gene controlling flowering time in *Arabidopsis*, encodes a protein containing RNA-binding domains. *Cell* 89, 737-745.
- Maliga P, Klessig DF, Cashmore AR, Gruissem W, Varner JE (eds). *Methods in Plant Molecular Biology: A Laboratory Course Manual*. Cold Spring Harbor. Laboratory Press, Cold Spring Harbor, NY. 1995.
- McConn, M., and Browse, J. (1996). The Critical Requirement for Linolenic Acid Is Pollen Development, Not Photosynthesis, in an *Arabidopsis* Mutant. *Plant Cell* 8, 403-416.
- McConn, M., Creelman, R.A., Bell, E., Mullet, J.E., and Browse, J. (1997). Jasmonate is essential for insect defense in *Arabidopsis*. *Proc Natl Acad Sci U S A* 94, 5473-5477.
- McGill University and Génome Québec Innovation Centre. Functional Genomics Platform. 740, Dr Penfield Avenue, Room 6300. Montréal (Québec) Canada.
- Michaels, S.D., and Amasino, R.M. (1999). FLOWERING LOCUS C encodes a novel MADS domain protein that acts as a repressor of flowering. *Plant Cell* 11, 949-956.
- Murashige T and Skoog F (1962) A revised medium for rapid growth and bioassays with tobacco tissue cultures. *Physiol Plant* 15(3): 473-497.
- Mouradov, A., Cremer, F. and Coupland, G. (2002). Control of Flowering Time: Interacting Pathways as a Basis for Diversity. *Plant Cell* 14 (90001): S111-130.
- Onouchi, H., Igeno, M.I., Perilleux, C., Graves, K., and Coupland, G. (2000). Mutagenesis of plants overexpressing CONSTANS demonstrates novel interactions among *Arabidopsis* flowering-time genes. *Plant Cell* 12, 885-900.
- Pelacho, A.M., and Mingo-Castel, A.M. (1991). Jasmonic Acid Induces Tuberization of Potato Stolons Cultured in Vitro. *Plant Physiol* 97, 1253-1255.
- Penninckx, I.A., Eggermont, K., Terras, F.R., Thomma, B.P., De Samblanx, G.W., Buchala, A., Metraux, J.P., Manners, J.M., and Broekaert, W.F. (1996). Pathogen-induced systemic activation of a plant defensin gene in *Arabidopsis* follows a salicylic acid-independent pathway. *Plant Cell* 8, 2309-2323.

- Poethig, R.S. (1990). Phase Change and the Regulation of Shoot Morphogenesis in Plants. *Science* 250, 923-930.
- Putterill, J., Robson, F., Lee, K., Simon, R., and Coupland, G. (1995). The *CONSTANS* gene of *Arabidopsis* promotes flowering and encodes a protein showing similarities to zinc finger transcription factors. *Cell* 80, 847-857.
- Quesada, V., Macknight, R., Dean, C., and Simpson, G.G. (2003). Autoregulation of FCA pre-mRNA processing controls *Arabidopsis* flowering time. *Embo J* 22, 3142-3152.
- Ranjan R, Lewak S. (1992) Jasmonic acid promotes germination and lipase activity in non-stratified apple embryos. *Physiol Plant*; 86:335–339.
- Rouse, D.T., Sheldon, C.C., Bagnall, D.J., Peacock, W.J., and Dennis, E.S. (2002). *FLC*, a repressor of flowering, is regulated by genes in different inductive pathways. *Plant J* 29, 183-191.
- Saugy, M., Mayor, G., and Pilet, P.E. (1989). Endogenous ABA in Growing Maize Roots: Light Effects. *Plant Physiol* 89, 622-627.
- Seo, H.S., Song, J.T., Cheong, J.J., Lee, Y.H., Lee, Y.W., Hwang, I., Lee, J.S., and Choi, Y.D. (2001). Jasmonic acid carboxyl methyltransferase: a key enzyme for jasmonate-regulated plant responses. *Proc Natl Acad Sci U S A* 98, 4788-4793.
- Shannon, S. and Meeks-Wagner, D. R. (1993). Genetic interactions that regulate inflorescence development in *Arabidopsis*. *Plant Cell* 5, 639-655.
- Sheldon, C.C., Burn, J.E., Perez, P.P., Metzger, J., Edwards, J.A., Peacock, W.J., and Dennis, E.S. (1999). The *FLF* MADS box gene: a repressor of flowering in *Arabidopsis* regulated by vernalization and methylation. *Plant Cell* 11, 445-458.
- Simon, R., Igeno, M.I., and Coupland, G. (1996). Activation of floral meristem identity genes in *Arabidopsis*. *Nature* 384, 59-62.
- Simpson, G.G., Gendall, A.R., and Dean, C. (1999). When to switch to flowering. *Annu Rev Cell Dev Biol* 15, 519-550.
- Smith, M., Moon, H., and Kunst, L. (2000). Production of hydroxy fatty acids in the seeds of *Arabidopsis thaliana*. *Biochem Soc Trans* 28, 947-950.

- Stelmach, B.A., Muller, A., Hennig, P., Gebhardt, S., Schubert-Zsilavecz, M., and Weiler, E.W. (2001). A novel class of oxylipins, sn1-O-(12-oxophytodienoyl)-sn2-O-(hexadecatrienoyl)-monogalactosyl Diglyceride, from *Arabidopsis thaliana*. *J Biol Chem* 276, 12832-12838.
- Stenzel, I., Hause, B., Miersch, O., Kurz, T., Maucher, H., Weichert, H., Ziegler, J., Feussner, I., and Wasternack, C. (2003). Jasmonate biosynthesis and the allene oxide cyclase family of *Arabidopsis thaliana*. *Plant Mol Biol* 51, 895-911.
- Stintzi, A., and Browse, J. (2000). The *Arabidopsis* male-sterile mutant, *opr3*, lacks the 12-oxophytodienoic acid reductase required for jasmonate synthesis. *Proc Natl Acad Sci U S A* 97, 10625-10630.
- Stintzi, A., Weber, H., Reymond, P., Browse, J., and Farmer, E.E. (2001). Plant defense in the absence of jasmonic acid: the role of cyclopentenones. *Proc Natl Acad Sci U S A* 98, 12837-12842.
- Sung, Z.R., and Takahashi, S. (2001). EMBRYONIC FLOWER2, a novel Polycomb group protein homolog, mediates shoot development and flowering in *Arabidopsis*. *Plant Cell* 13, 2471-2481.
- Swiatek, A., Van Dongen, W., Esmans, E.L., and Van Onckelen, H. (2004). Metabolic fate of jasmonates in tobacco bright yellow-2 cells. *Plant Physiol* 135, 161-172.
- Taiz L., and Zeiger E. (2006). *Plant Physiology*, Fourth edition. Sinauer Associates. Sunderland, MA.
- Tamayo, P., Slonim, D., Mesirov, J., Zhu, Q., Kitareewan, S., Dmitrovsky, E., Lander, E., and Golub, T. (1999). Interpreting patterns of gene expression with self-organizing maps. *PNAS*, 96:2907-2912
- Ueda, R. Ogata, S., Morrissey, DM, Finstad, CL, Szkudlarek, J., Whitmore, WF, Oettgen, HF, Lloyd, KO, and Old, LJ (1981) Cell surface antigens of human renal cancer defined by mouse monoclonal antibodies: Identification of tissue-specific kidney glycoproteins. *Proc. Natl. Acad. Sci. USA* 78:5122-5126.
- van der Fits, L. and Memelink, J. (2000). ORCA3, a Jasmonate-Responsive Transcriptional Regulator of Plant Primary and Secondary Metabolism. *Science* 289, 295 – 297.
- Valverde, F., Mouradov, A., Soppe, W., Ravenscroft, D., Samach, A., and Coupland, G. (2004). Photoreceptor regulation of CONSTANS protein in photoperiodic flowering. *Science* 303, 1003-1006.

- Vargas, F., Frerot, O., Brion, F., Trung Tuong, M.D., Lafitte, A., and Gulat-Marnay, C. (1994). 3'-Phosphoadenosine 5'-phosphosulfate biosynthesis and the sulfation of cholecystinin by the tyrosylprotein-sulfotransferase in rat brain tissue. *Chem Biol Interact* 92, 281-291.
- Vick, B.A., and Zimmerman, D.C. (1983). The biosynthesis of jasmonic acid: a physiological role for plant lipoxygenase. *Biochem Biophys Res Commun* 111, 470-477.
- Webb, D.T. (1983) Nodulation in Light and Dark-Grown *Macrozamia communis* L. Johnson Seedlings in Sterile Culture, *Ann. Bot.*, 52: 543-547.
- Weber, H. (2002). Fatty acid-derived signals in plants. *Trends Plant Sci* 7, 217-224.
- Weberling, F. Morphology of flowers and inflorescences. Cambridge University Press. Cambridge (United Kingdom). 1989.
- Weinshilboum, R. M., Otterness, D. M., Aksoy, I. A., Wood, T. C., Her, C., and Raftogianis, R. B. (1997). Sulfation and sulfotransferases 1: Sulfotransferase molecular biology: cDNAs and genes. *FASEB J.* 11, 3-14.
- Wenkel S, Turck F, Singer K, Gissot L, Le Gourrierc J, Samach A, Coupland G (2006) CONSTANS and the CCAAT box binding complex share a functionally important domain and interact to regulate flowering of Arabidopsis. *Plant Cell* 18: 2971–2984
- Wilson P. 1992. On inferring hybridity from morphological intermediacy. *Taxon* 41: 11-23.
- Yoshihara, T., Omer, E.-S. A., Koshino, H., Sakamura, S., Kikuta, Y., and Koda, Y. (1989) Structure of a tuber-inducing stimulus from potato leaves (*Solanum tuberosum* L.). *Agric. Biol. Chem.* 53, 2835-2837.
- Xu, J. H., Shen, J. L., Miller Jr., J. H., and Ting, C. S. 1994. Superconducting Pairing Symmetry and Josephson Tunneling. *Phys. Rev. Lett.* 73, 2492 - 2495.
- Zeevaart, J.A.D. (1958). Flower formation as studied by grafting. *Meded. Landbouwhoges. Wagening.* 58(3), 1–88.
- Zimmermann P., Hirsch-Hoffmann M., Hennig L., and Gruissem, W. (2004). GENEVESTIGATOR: Arabidopsis Microarray Database and Analysis Toolbox. *Plant Physiology* 136 1, 2621-2632.